CPT-Based Axial Capacity Design Method for Driven Piles in Clay

Lehane, Barry M.; Liu, Zhongqiang; Bittar, Eduardo J.; Nadim, Farrokh; Lacasse, Suzanne; Bozorgzadeh, Nezam; Jardine, Richard; Ballard, Jean Christophe; Gavin, Kenneth; More Authors

DOI
10.1061/(ASCE)GT.1943-5606.0002847

Publication date
2022

Document Version
Final published version

Published in
Journal of Geotechnical and Geoenvironmental Engineering

Citation (APA)
Lehane, B. M., Liu, Z., Bittar, E. J., Nadim, F., Lacasse, S., Bozorgzadeh, N., Jardine, R., Ballard, J. C., Gavin, K., & More Authors (2022). CPT-Based Axial Capacity Design Method for Driven Piles in Clay. *Journal of Geotechnical and Geoenvironmental Engineering*, *148*(9), Article 04022069. https://doi.org/10.1061/(ASCE)GT.1943-5606.0002847

ASCE

CPT-Based Axial Capacity Design Method for Driven Piles in Clay

Barry M. Lehane[1]; Zhongqiang Liu[2]; Eduardo J. Bittar[3]; Farrokh Nadim[4]; Suzanne Lacasse[5]; Nezam Bozorgzadeh[6]; Richard Jardine[7]; Jean-Christophe Ballard[8]; Pasquale Carotenuto[9]; Kenneth Gavin[10]; Robert B. Gilbert, F.ASCE[11]; Jens Bergan-Haavik[12]; Philippe Jeanjean, F.ASCE[13]; and Neil Morgan[14]

Abstract: There are clear advantages in the establishment of reliable, direct cone penetration test (CPT) based methods for assessment of the axial capacity of driven piles. These advantages motivated the formation of a joint industry project (JIP) under the management of the Norwegian Geotechnical Institute (NGI), which initially led to the creation of a unified database of high-quality pile load tests in sand and clay. The unified database has the consensus approval of representatives of the profession and personnel in multiple companies from the offshore energy sector. This paper presents a component of the research from the second phase of the JIP, which had the objective of developing a new CPT-based method for driven piles in clay to unify several CPT-based methods that are in use today. First, a rational basis for the CPT-based formulation is described, using trends from instrumented pile tests; the description facilitates an understanding of the approach and illustrates its empirical nature and limitations. The unified database was used to calibrate the formulation and it led to good predictions for an independent database of pile load tests and for measured distributions of shaft friction. **DOI: 10.1061/(ASCE)GT.1943-5606.0002847.**

[1]Professor, School of Engineering, Univ. of Western Australia, Crawley, WA 6009, Australia (corresponding author). ORCID: https://orcid.org/0000-0003-0244-7423. Email: Barry.Lehane@uwa.edu.au

[2]Senior Engineer, Norwegian Geotechnical Institute, P.O. Box 3930 Ullevål Stadion, N-0806 Oslo, Norway. Email: Zhongqiang.Liu@ngi.no

[3]Ph.D. Student, School of Engineering, Univ. of Western Australia, Crawley, WA 6009, Australia. ORCID: https://orcid.org/0000-0002-1377-7965. Email: eduardo.bittarmarin@research.uwa.edu.au

[4]Technical Director, Norwegian Geotechnical Institute, P.O. Box 3930 Ullevål Stadion, N-0806 Oslo, Norway. Email: Farrokh.Nadim@ngi.no

[5]Expert Advisor, Norwegian Geotechnical Institute, P.O. Box 3930 Ullevål Stadion, N-0806 Oslo, Norway. Email: Suzanne.Lacasse@ngi.no

[6]Professor, Dept. of Civil and Environmental Engineering, Imperial College, London SW7 2BU, UK. Email: r.jardine@imperial.ac.uk

[7]Visiting Academic, Norwegian Geotechnical Institute, P.O. Box 3930 Ullevål Stadion, N-0806 Oslo, Norway. ORCID: https://orcid.org/0000-0001-7147-5909. Email: Nezam.bozorgzadeh@ngi.no

[8]Principal Engineer, Fugro Belgium, Rue du Bosquet, 1348 Louvain-la-Neuve, Belgium. Email: jc.ballard@fugro.com

[9]Senior Engineer, Norwegian Geotechnical Institute, P.O. Box 3930 Ullevål Stadion, N-0806 Oslo, Norway. Email: Pasquale.Carotenuto@ngi.no

[10]Professor, Faculty of Civil Engineering and Geosciences Building, Delft Univ. of Technology, 23 Stevinweg 1, P.O. Box 5048 2628, Delft, The Netherlands. Email: k.g.gavin@tudelft.nl

[11]Professor, Dept. of Civil, Architectural and Environmental Engineering, Univ. of Texas at Austin, TX 78712. Email: bob_gilbert@mail.utexas.edu

[12]Principal Engineer, DNV AS, Veritasveien 1, Høvik 1363, Norway. ORCID: https://orcid.org/0000-0002-2625-8523. Email: jens.bergan.haavik@dnv.com

[13]Senior Advisor, BP America, 501 Westlake Park Boulevard, Houston, TX 77079. Email: Philippe.Jeanjean@bp.com

[14]Principal Engineer, Lloyd's Register EMEA, Kingswells Causeway, Aberdeen AB15 8PJ, UK. Email: Neil.Morgan@lr.org

Note. This manuscript was submitted on November 19, 2020; approved on April 8, 2022; published online on July 1, 2022. Discussion period open until December 1, 2022; separate discussions must be submitted for individual papers. This paper is part of the ***Journal of Geotechnical and Geoenvironmental Engineering***, © ASCE, ISSN 1090-0241.

Introduction

Estimates of the axial capacity of driven piles in clay depend primarily on the assessment of shaft friction (τ_f), which typically represents a major proportion of the axial capacity. The alpha (α) design method proposed by American Petroleum Institute (API) (2011) is currently the most common approach used to assess τ_f, and it assumes that τ_f varies directly with the triaxial compression unconsolidated undrained (UU) shear strength of the clay (s_u^{UU}) via an α (or adhesion) factor. The α value is expressed as an empirical function of the undrained strength ratio (s_u^{UU}/σ'_{v0}) that has been determined from a best fit to capacities measured in a database of pile load tests (Randolph and Murphy 1985). The application of α approaches usually require the drilling and sampling of boreholes and subsequent undrained strength tests on a representative number of nominally undisturbed samples. The cost of such investigations coupled with the discrete nature of sampling and the well-known variability in s_u data due to sampling disturbance and other effects prompted this investigation into the new cone penetration test–(CPT) based method presented in this paper.

Relationships between shaft friction and the CPT-measured and -corrected cone end resistances (q_c and q_t) for driven piles in clay have been proposed for many years—for example, Bustamante and Gianeselli (1982), Almeida et al. (1996), Lehane et al. (2000, 2013), Eslami and Fellenius (1997), and Niazi and Mayne (2016). This paper builds upon this previous research and presents a new CPT-based method that was calibrated using a new database of pile load tests that was compiled by a team of experts working for a large joint industry project (JIP) (Lehane et al. 2017). The sand and the clay-pile test databases compiled for this JIP are referred to as unified databases, because they comprise the most reliable pile tests from a number of databases and were reviewed in depth to ensure that they had the consensus approval of the profession. The creation of a sand database already led to the development of a new CPT-based method for driven piles in sand (Lehane et al. 2020) that replaced the previously recommended earth pressure

design approach in the draft version of the next edition of ISO 19901-4 (ISO 1996), planned for publication in 2021.

This paper first presents an analysis of results from instrumented pile test data and numerical research that provides a rational basis for CPT-based formulations for axial pile capacity in clay and facilitates an understanding of the limitations of these formulations. The ability of a range of formulations to predict the capacities of piles in the unified database was examined to establish a final set of recommended equations for shaft friction and end bearing. The reliability of these equations was assessed by comparing their predictions for the capacities of piles to those in a separate test database that was compiled for this study and with distributions of shaft frictions measured on well-instrumented test piles.

Basis for Formulation for Shaft Friction

General Trends Indicated by Instrumented Closed-Ended Piles

The stress changes that take place during the three stages in the life of a driven pile (i.e., installation, equalization, and load testing) ultimately control the magnitude of the shaft friction that can be developed when a pile is in service. These changes are illustrated for the case of a lightly overconsolidated clay in Fig. 1, which shows average data measured at the shaft of a jacked 6-m-long, 102-mm-diameter pile in Bothkennar clay (Lehane and Jardine 1994a). The trends shown in Fig. 1 are typical of data measured in other instrumented pile tests reported by Azzouz and Morrison (1988), NGI (1988a, b) and Coop and Wroth (1989). The subscripts i and c used in the following refer to installation and following equalization (consolidation), respectively.

Fig. 1(a) shows that radial stresses measured at any given depth during installation (σ_{ri}) are smaller than, but proportional to, the CPT q_t resistances. These σ_{ri} data also vary with the distance of the radial stress sensor above the tip (h) and, in any given soil horizon, are about 40% of the q_t value at four pile diameters from the tip ($h/D = 4$) and about 30% of q_t at $h/D \geq 14$. Installation excess pore pressure ratios ($\Delta u_i/\sigma'_{v0}$) at this site varied from about 3 at $h/D = 1.5$ to about 2.1 at $h/D \geq 16$. After the pile reached the required embedment, as shown in Fig. 1(b), excess pore pressures dissipated, radial total stresses (σ_r) decreased, and radial effective stresses increased (σ'_r) over several days to reach the final fully equalized radial effective stress of σ'_{rc}. In this example, σ'_{rc} is about three times the radial effective stress acting on the shaft shortly after installation (σ'_{ri}). During load testing after full equalization, Fig. 1(c) shows that radial effective stresses decrease to values at peak shear stresses (σ'_{rf}) that are about 20% less than σ'_{rc}. The maximum shaft friction (τ_f) is controlled, through Coulomb's friction law, by the radial effective stress at failure (σ'_{rf}) and the average clay–pile interface friction angle (δ) of 29°; this δ value is closely comparable to angles measured in ring interface shear tests on Bothkennar clay using a rough steel interface; see Lehane and Jardine (1992).

These stages in the life of a pile can be written in terms of radial total stresses (σ_r) normalized by the corrected cone resistance (q_t) using the following stress coefficients, where u_0 is the hydrostatic or ambient pore pressure

$$S_i = (\sigma_{ri} - u_0)/q_t \tag{1}$$

$$S_c = (\sigma_{rc} - u_0)/q_t = \sigma'_{rc}/q_t \tag{2}$$

The loading coefficient is the ratio of the radial effective stress at peak shear stress (σ'_{rf}) to the equalized radial effective stress (σ'_{rc})

$$f_L = \sigma'_{rf}/\sigma'_{rc} \tag{3}$$

Jardine et al. (2005) and many others have confirmed the validity of Coulomb's friction law at the loading rates adopted in typical static load tests. Assuming Coulomb's friction law, Eqs. (1)–(3) then lead to the following expression for shaft friction τ_f, which gives τ_f as a direct function of the corrected cone resistance q_t, the three stress coefficients, and the interface friction angle δ

$$\tau_f = \sigma'_{rf} \tan\delta = q_t S_i (S_c/S_i) f_L \tan\delta \tag{4}$$

The relationship between τ_f and q_t given in Eq. (4) was examined first using data recorded for the Imperial College instrumented pile (ICP) in London clay, Cowden till, Bothkennar clay, and Pentre

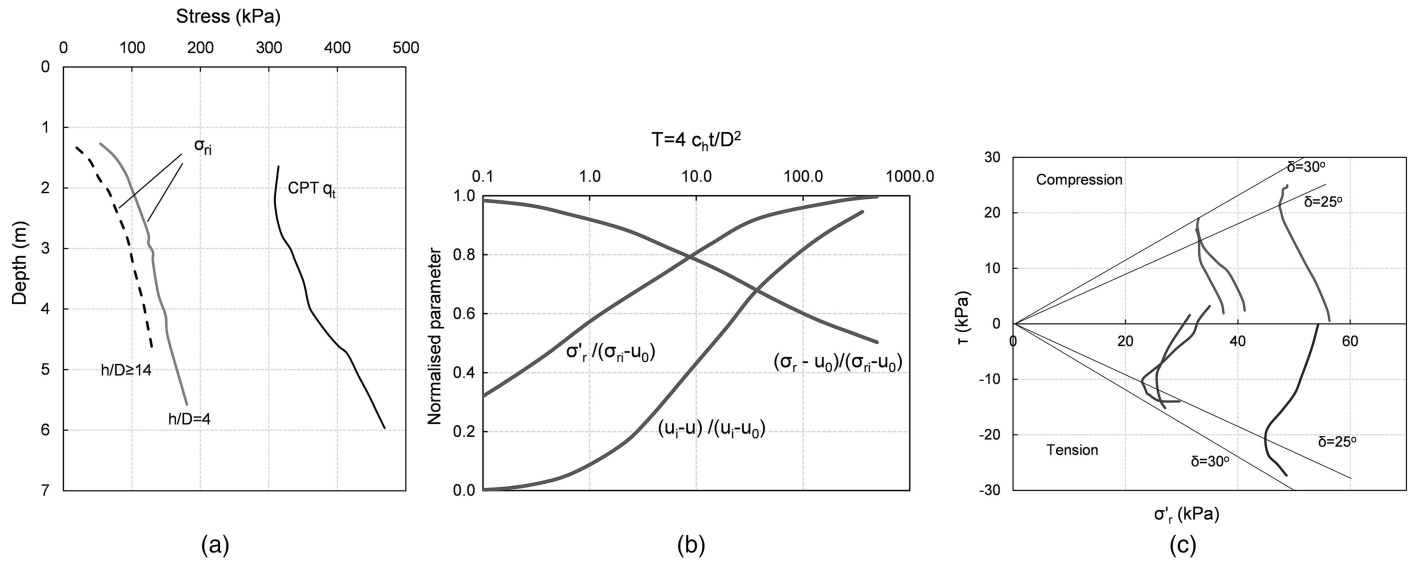

Fig. 1. Responses recorded in low-OCR clay: (a) radial total stresses during installation; (b) normalized stress changes during equalization; and (c) shear stress variations with radial effective stress during pile load testing. (Data from Lehane 1992.)

J. Geotech. Geoenviron. Eng., 2022, 148(9): 04022069

clayey silt (Bond and Jardine 1991; Lehane and Jardine 1994a, b; Jardine et al. 2005). These experiments showed that the S_i measurements at each site could be represented as a unique function of the normalized distance above the pile tip (h/D) with the following format, where A and c are fitting parameters

$$S_i = (\sigma_{ri} - u_0)/q_t = A(h/D)^{-c} \quad (5)$$

An illustration of the suitability of the format of Eq. (5) is provided using data from Lehane and Jardine (1994b) in Fig. 2, which reveals a clear similarity between the q_t profile measured in glacial till at Cowden, UK [Fig. 2(b)], and corresponding ICP radial stress profiles recorded during installation by instruments located at $h/D = 4$, 14, and 25 [Fig. 2(a)]. Radial stresses for the three piles installed from a 2.5-m-deep borehole varied by about 10% from mean values at any given instrument position. The range of all σ_{ri} data recorded by the four piles, presented as a variation of S_i with h/D, is shown in Fig. 2(c), which also plots the mean trend line (with correlation coefficient $R^2 = 0.82$) corresponding to the A and c coefficients provided in Table 1. Lehane (1992) showed that the equivalent variability about mean trend lines determined for σ_{ri} data for London clay and Bothkennar clay were 25% and 6%, respectively.

Mean variations of S_i with h/D recorded by the ICP are plotted in Fig. 3(a), in which considerable differences between the trends in each clay are apparent. The best-fit average values of A and c corresponding to these trend lines are provided in Table 1 and indicate a significant dependence of c on clay type. The mean overconsolidation ratio (OCR) and plasticity index (I_p) at these sites are also provided in Table 1. A clear dependence of S_i on h/D was observed at a much reduced scale by Li and Lehane (2012) using a 9-mm-wide pile, confirming the suitability of pile diameter (or width) to normalize the distance from the pile tip (h).

The corresponding trends of normalized shaft friction (τ_f/q_t) are plotted in Fig. 3(b) and were derived using Eq. (4) and the mean A, c, S_c/S_i, f_L, and δ values listed in Table 1, which were determined from the Imperial College experiments. These average coefficients did not indicate a systematic dependence on depth or pile length at the respective sites. It is evident that the spread of τ_f/q_t variations with h/D is lower than that of S_i in Fig. 3(a), and τ_f/q_t ratios at a fixed h/D typically vary by less than 25% from the mean trend of the four clays.

Further instrumented pile test data are shown in Fig. 4 to allow a comparison of results obtained in three lightly overconsolidated clays, namely Onsøy, Lierstranda, and Bothkennar clays. The test results in both Onsøy and Lierstranda clays, which were reported in NGI (1988a, b) and Karlsrud et al. (1993b), were obtained using eight 219-mm-diameter piles driven to final penetrations of between 15 m and 35 m. Each pile was equipped with a pair of radial stress sensors located at three levels, 5m apart. The CPT q_t profiles at Bothkennar and Onsøy varied approximately linearly with depth with a gradient of 40 kPa/m, while q_t values at Lierstranda also varied linearly with depth but with a gradient of about 50 kPa/m.

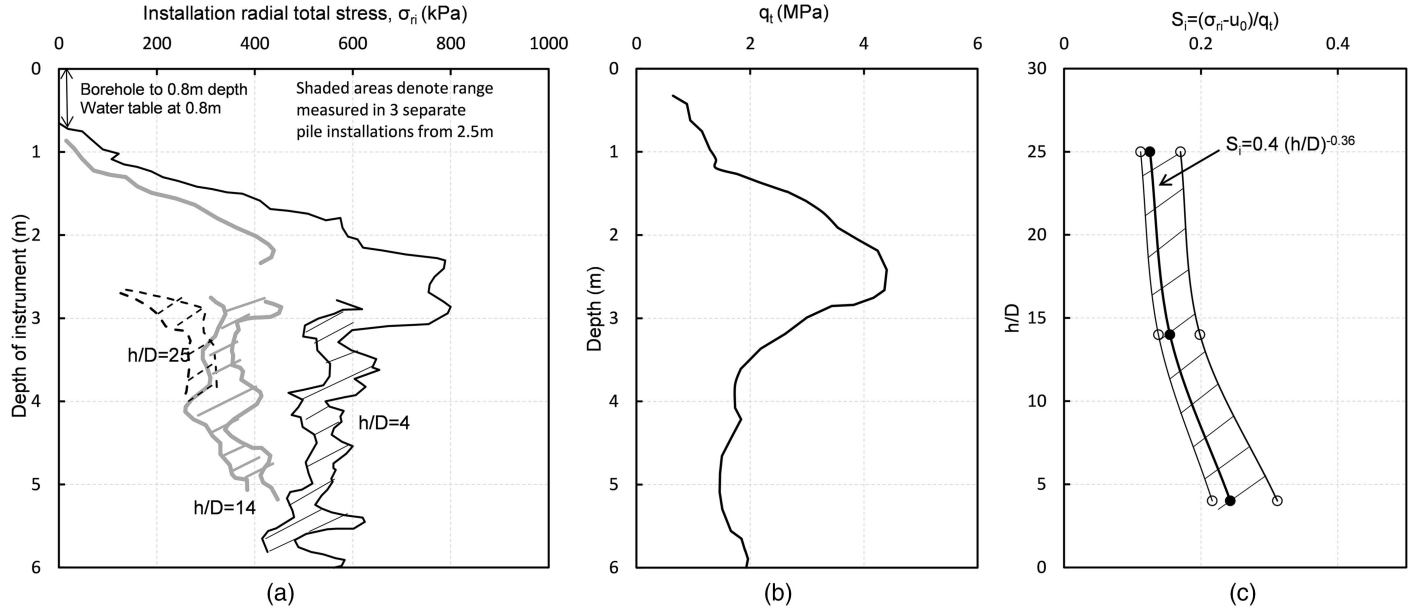

Fig. 2. Instrumented pile tests at Cowden: (a) radial stresses recording during installation; (b) CPT resistance profile; and (c) variation of S_i with h/D.

Table 1. Coefficients measured in instrumented pile tests

Clay	OCR	I_p (%)	A	c	S_c/S_i	f_L	δ (degrees)
Cowden till	10	21	0.40	0.36	0.80	0.80	22
London clay	30	50	0.65	0.59	1.00	1.00	13
Bothkennar clay	1.7	47	0.50	0.24	0.43	0.80	29
Pentre silt	1.8	16	0.62	0.45	0.65	0.92	20
Onsøy clay	1.3	43	0.40	0.15	0.32	0.81	24
Lierstranda clay	1.2	16	0.48	0.28	0.15	0.60	26.5

Note: Definitions of coefficients are provided in Eqs. (1)–(3), and (5).

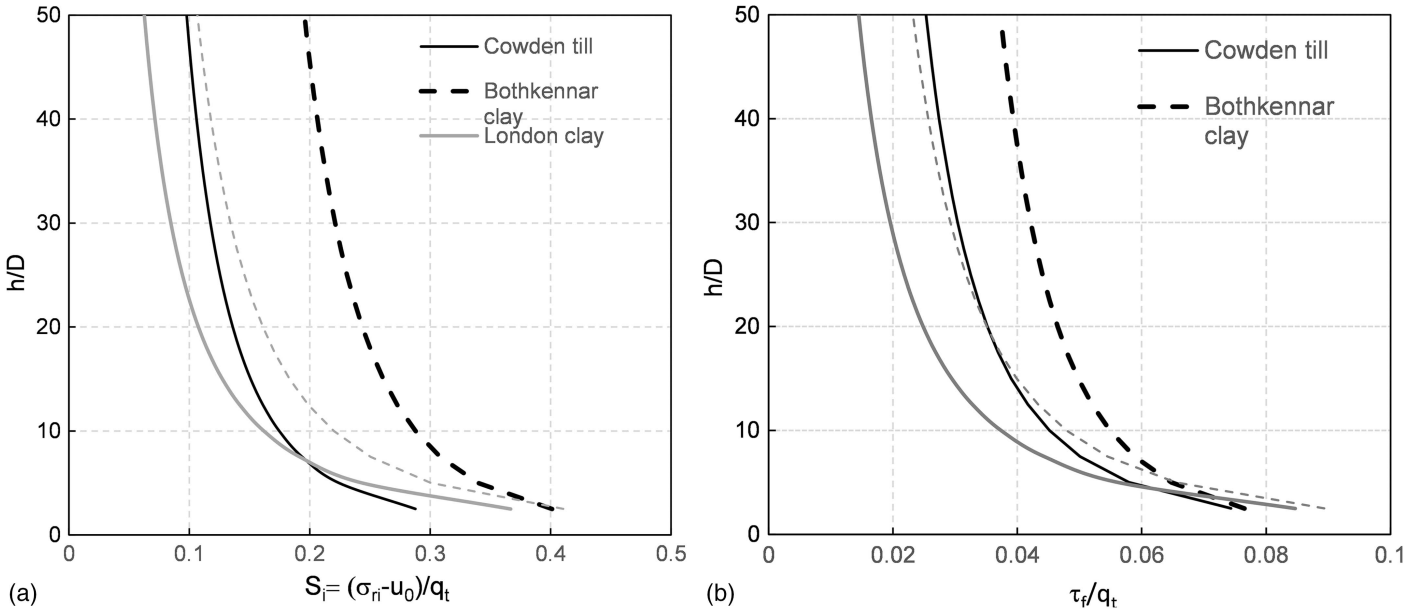

Fig. 3. Variation of (a) normalized installation radial stress S_i; and (b) normalized peak friction in four different clays (recorded by the Imperial College instrumented pile).

Best-fit A and c coefficients derived from the measured S_i data are also listed in Table 1, and although these differ in magnitude, it is evident from the variations of S_i with h/D shown in Fig. 4(a) that a broadly comparable S_i relationship with h/D exists for these three low-OCR clays. However, as seen in Figs. 4(b and c), values of S_c/S_i and f_L are not similar, with much lower values of these parameters being recorded in the Lierstranda clay.

Numerical analyses performed using the strain path method (SPM) and the E3 model of the Massachusetts Institute of Technology (MIT-E3) constitutive model reported by Whittle and Baligh (1988), Azzouz et al. (1990), and others, have shown that clay sensitivity S_t and OCR have a dominant effect on the relaxation of total stresses during pore pressure equalization and, hence, the S_c/S_i ratio. These analyses are supported by the measured ratios given in Table 1, which indicate S_c/S_i values between 0.8 and 1.0 in the high-OCR Cowden till and London clay and between 0.15 and 0.43 in the three low-OCR clays considered. Of particular note, is the much lower S_c/S_i value in Lierstranda clay. The CPT friction ratio data indicate that the Lierstranda clay has a sensitivity S_t of about 9, compared with S_t values of 3.5 and 6.0 for Bothkennar and Onsøy clays, respectively. The CPT data for the Lierstranda clay plot close to or within Zone 1 of the soil behavior type (SBT) chart (Robertson 2009), denoting a sensitive clay, while the Bothkennar and Onsøy clays classify as typical silty clays, within Zone 3.

As seen in Table 1, the average f_L value for Lierstranda clay is also lower than the values for less sensitive clays, indicating that greater reductions in radial effective stress σ_r' occurred during static load tests in this material. Greater reductions in σ_r' also occurred during undrained direct simple shear (DSS) tests on intact samples of Lierstranda clay compared with Onsøy and Bothkennar clays, but these reductions were not as marked as those measured in the pile tests.

The compounding effect of low S_c/S_i and f_L ratios leads to very low τ_f/q_t ratios in Lierstranda clay, although its S_i and δ values are comparable to those of the other low-OCR clays. Such low ratios are apparent in Fig. 5, which plots all variations of τ_f/q_t with h/D determined using Eq. (4) and the average coefficients in all clays (Table 1). The variations of τ_f/q_t with h/D are broadly similar, apart from those for the Lierstranda clay, and can be generally represented to within 20% by the following mean trend line, which is also shown in the figure

$$\tau_f = 0.08 q_t (h/D)^{-0.3} \quad h/D > 0 \tag{6}$$

The Lierstranda test data can be represented using the same format if a sensitivity factor F_{st} is applied to Eq. (6), that is

$$\tau_f = 0.08 F_{st} q_t (h/D)^{-0.3} \quad h/D > 0 \tag{7}$$

where $F_{st} = 0.3$ in Lierstranda clay (which is in Zone 1 of the SBT chart) and unity in typical clays (i.e., in Zones 2, 3, and 4 of the SBT chart).

Eq. (7), which was derived solely from instrumented pile tests, provides an indication of a potential formulation for a CPT-based method for closed-ended piles. However, when seeking a best-fit formulation for the unified database of pile load tests, it is important to recognize that the similarity of the relationship for the soils with $F_{st} = 1.0$ arises because of compensating effects in Eq. (4) of the parameters given in Table 1.

The dependence of τ_f on h/D in Eq. (7) is consistent with considerations of length effects dating back to the reduction of the adhesion factor (α) with L/D proposed by Semple et al. (1984) and Kolk and van der Velde (1996). This dependence has been predicted numerically (but to a lesser extent) using the SPM with the MIT-E3 soil model (Whittle 1991). Effects of progressive failure for long piles (e.g. Kraft et al. 1981) add to the h/D dependence in Eq. (7). The effect of clay sensitivity, which emerged from the same SPM/MIT-E3 analyses, was employed explicitly in formulations for τ_f involving OCR proposed by Lehane et al. (1994) and Jardine et al. (2005).

Open-Ended Piles

The lower levels of soil displacement associated with the installation of open-ended piles compared to closed-ended piles might be expected to lead to lower shaft friction, as is the case for piles in sand (e.g., Gavin and Lehane 2003). However, empirical

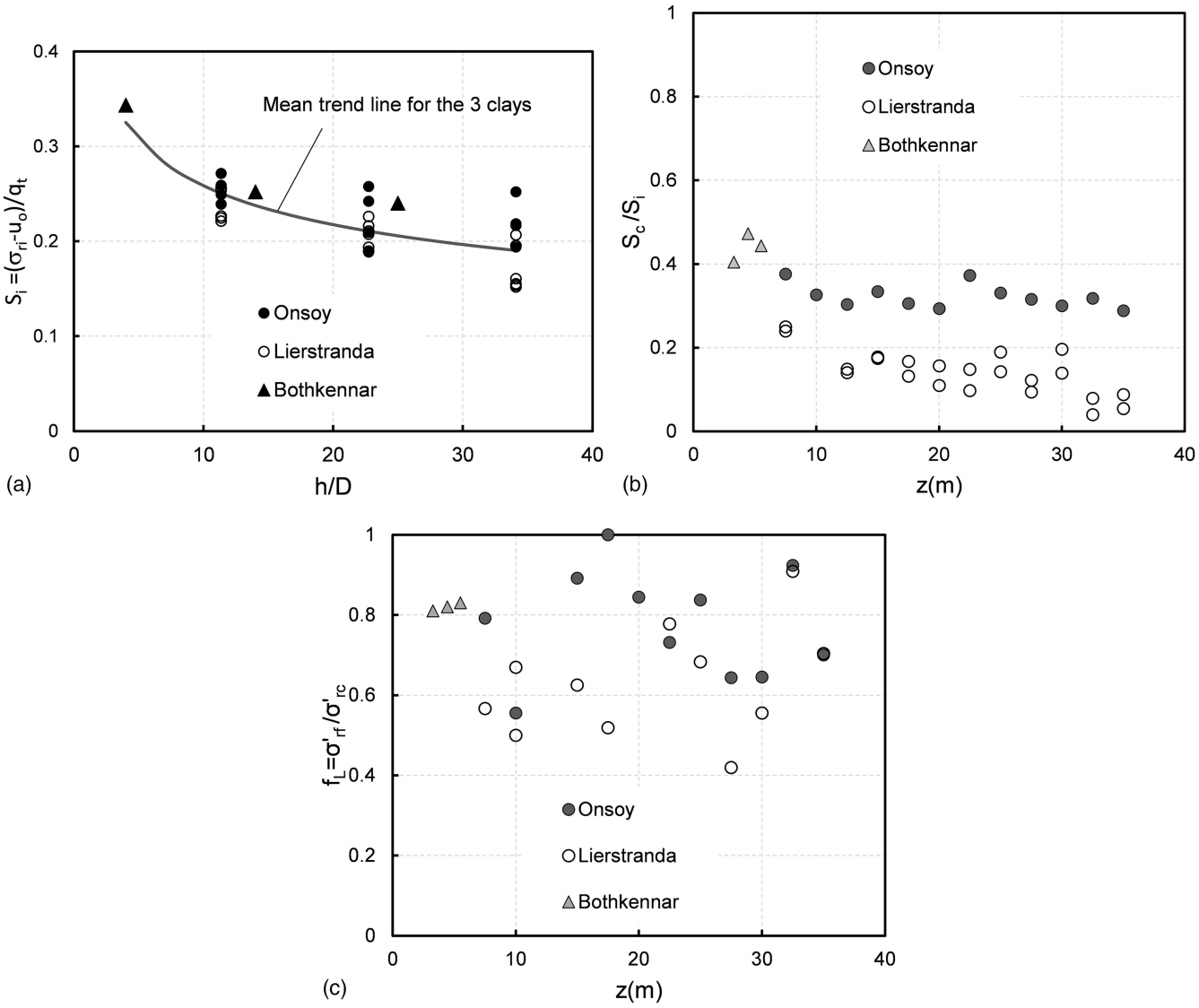

Fig. 4. Stress coefficients recorded in Onsøy, Lierstranda, and Bothkennar clays. (Data from NGI 1988a, b; Lehane and Jardine 1994a.)

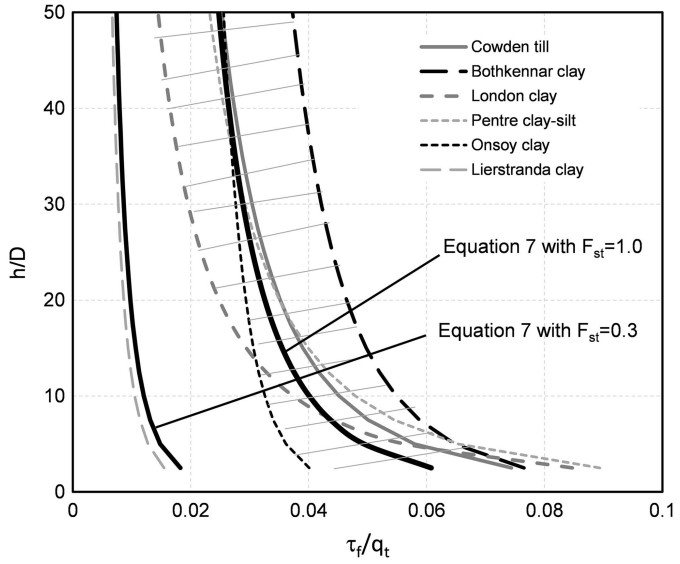

Fig. 5. Average variations of τ_f/q_t ratios with h/D inferred from instrumented data in six clays.

correlations such as those proposed by Bustamante and Gianeselli (1982) and Karlsrud et al. (2005) have suggested that there is no dependence on the plugging condition in low-OCR clays but rather that friction in stiff or high-OCR clays may be lower for open-ended piles. Miller and Lutenegger (1997) measured lower friction for open-ended piles in high-OCR clay and observed lower friction at lower degrees of plugging during installation in cases in which plugging was described by the plug length ratio (PLR).

Therefore, following a logic similar to that adopted for the development of the CPT-based method for piles in sand using the unified database (Lehane et al. 2020), effects of soil displacement can be examined via an extension of Eq. (5) by assuming that the normalized installation total stress S_i depends on h/D (as for a closed-ended pile) and the effective area ratio A_{re}

$$S_i = AA_{re}^b(h/D)^{-c} \tag{8}$$

where b is a fitting parameter; and A_{re} represents the relative degree of displacement compared to a closed-ended pile and is defined as a function of internal pile diameter D_i and PLR

$$A_{re} = 1 - \mathrm{PLR}(D_i/D)^2 = (D_{eq}/D)^2 \tag{9a}$$

J. Geotech. Geoenviron. Eng., 2022, 148(9): 04022069

$$\text{PLR} = \tan h\left[0.3\left(\frac{D_i}{d_{\text{CPT}}}\right)^{0.5}\right]; \quad d_{\text{CPT}} = 35.7 \text{ mm} \tag{9b}$$

PLR can be estimated from Eq. (9*b*), which is based on available plugging data for piles in clay (Lehane et al. 2017) and is zero for closed-ended piles. The level of partial plugging of a pipe pile can also be described by the term D_{eq}, which is the diameter of an equivalent closed-ended pile leading to the same level of soil displacement.

Eq. (8) is consistent with the lateral stress data recorded in low-OCR clay by Doherty and Gavin (2011) during the installation of (one of the very few) instrumented pipe piles in clay. The same set of experiments showed that the values of S_c/S_i, f_L, and δ were independent of the pile end condition. The potential effects of the clay OCR on S_i, referred to previously, are not considered explicitly in the assessment of best-fit formulations due to a shortage of related information.

The pile design method proposed by Jardine and Chow (1996) employs the term D^* to reflect the lower level of displacement induced during installation of a pipe pile

$$\begin{aligned} D^* &= (D^2 - D_i^2)^{0.5} \quad \text{for an open-ended pile} \\ D^* &= D \quad \text{for a closed-ended pile} \end{aligned} \tag{10}$$

The value of D^* is equal to D_{eq} when PLR = 1, and the expression corresponding to Eq. (8) is

$$S_i = A(h/D^*)^{-c} \tag{11}$$

The format of Eq. (11) is consistent with numerical analyses performed by Chin (1986), who predicted similar strain fields around closed- and (nonplugging) open-ended piles when distances from the pile are normalized by D^*. Xu et al. (2006) showed that the lateral stresses generated during installation of 1.02-m-diameter pipe piles and a 250-mm-square precast (closed-ended) pile have the same relationship with q_t and h/D^*. Eq. (11) was therefore also examined in the calibration of the database, because it represents a useful simplification of Eq. (8), given the approximate nature of the equation for PLR.

Loading Direction Coefficient f_D

The loading direction coefficient f_D is defined as the ratio of the ultimate shaft friction developed in tension to the friction developed in compression. This coefficient is best assessed by comparing values of τ_f developed in first-time compression and tension load tests on identical piles. Such comparisons have indicated f_D values of unity for piles in Kinnegar clay (McCabe and Lehane 2006), Bothkennar clay (Lehane and Jardine 1994a), London clay (Bond and Jardine 1991), Haga clay (Karlsrud and Haugen 1984), and Merville clay (Benzaria et al. 2012). However, f_D values measured in Cowden till (Lehane and Jardine 1994b) and Pentre clayey silt (Chow 1997) were 0.8 and 1.1, respectively. On this basis, a best-estimate f_D value of unity was adopted, although the optimization studies considered in the following also investigated other f_D values.

Basis for Formulation for End Bearing

The end bearing capacity of compression piles in clay usually represents a small fraction of the total capacity. This low relative contribution is reflected by the scarcity of research into the end bearing of driven piles in clay, particularly pipe piles. API (2011) recommends taking the lesser of the internal friction (calculated using the formulation for external friction) and the plugged end bearing, assumed to equal $9s_u$; this relationship equates to $0.75q_t$, for a typical CPT cone factor of 12 when relating cone resistance to undrained shear strength in triaxial compression. The plugged end bearing is almost always less than the calculated internal friction for typical piles with $L/D > 5$; therefore, the database analysis did not consider internal friction explicitly.

The few reliable cases that have measured the end bearing of closed-ended piles in clay indicated an end bearing at a pile movement of 10% of the pile diameter ($q_{b0.1}$) of about 80% of corrected cone resistance at the pile tip level (q_t). This proportion of q_t is similar to that proposed by Jardine and Chow (1996) and comparable to the recommendations of API (2011) and Van Dijk and Kolk (2011).

Doherty and Gavin (2011) presented a unique set of measurements involving a twin-walled instrumented pile that enabled separation of the average stress at the base of the plug and the stress on the annulus during pile installation. All installation data recorded can be represented by the following equation, in which A_{re} is given by Eq. (9)

$$q_{b0.1} = [0.2 + 0.6A_{re}]q_t \tag{12}$$

Eq. (12) implies that the undrained end-bearing capacity of a large offshore pile is approximately $0.2q_t$ (as A_{re} approaches zero) and is $0.8q_t$ for closed-ended piles. However, the capacities of piles in the unified database were measured in static load tests on relatively small diameter piles. Many of these pipe piles exhibited partial plugging during installation and also had a greater potential for drainage during the tests compared to closed-ended piles. Jardine et al. (2005) and Frank (2017) recommended $q_{b0.1}/q_t$ ratios for these smaller piles under load testing conditions of 0.4 and 0.35, respectively.

On the basis of the foregoing, the following equations were considered to provide a reasonable estimate of the end bearing mobilized by the database piles in static load tests (noting that the mean contribution to compression capacity of the end bearing of the database piles evaluated using these expressions was less than 15%)

$$q_{b0.1} = 0.8q_t \quad \text{(closed-ended pile)} \tag{13a}$$

$$q_{b0.1} = 0.4q_t \quad \text{(open-ended pile)} \tag{13b}$$

The Unified Database

A full description of the unified database in clay is provided in Lehane et al. (2017). A total of 300 pile load tests was examined, but only 49 tests with CPT data were selected based on stringent selection criteria explained in Lehane et al. (2017). These criteria included: (1) piles had to be driven with a minimum diameter of 200 mm and length of 5 m; (2) more than 75% of the shaft friction was provided by clay layers; (3) good quality CPT data were available close to the pile test; (4) the degree of consolidation prior to load testing was in excess of 80%, and only first-time tests were considered; (5) load-displacement data were provided for each test pile up to a pile head displacement of $D/10$; and (6) the loading rate was slow, with ultimate capacity typically attained a number of hours after the test start. A test database was compiled for the present study and followed these key criteria apart from allowing jacked piles and piles with smaller diameters and shorter lengths.

Details of the pile load tests in the unified database are provided in Tables 2 and 4, while details for the test database are presented in Table 3. The tables give details on the pile configurations, end conditions, loading direction, equalization time (t_{eq}), maximum

Table 2. Details of pile tests in unified database

No.	Site	Test name	Type	Borehole depth (m)	Tip depth (m)	t_{eq} (days)	D (m)	D_i (m)	L/D	Reference
1	Onsøy	A1-02	CET	5.0	15	26	0.22	—	45.7	Karlsrud et al. (1993b); and NGI (1988b)
2	Onsøy	A3-02	CET	20.0	30	54	0.22	—	45.7	Karlsrud et al. (1993b); and NGI (1988b)
3	Onsøy	B1-02	OET	5.0	15	81	0.81	0.79	12.3	Karlsrud et al. (1993b); and NGI (1988b)
4	Onsøy	C1-02	CET	5.0	35	50	0.22	—	137.0	Karlsrud et al. (1993b); and NGI (1988b)
5	Onsøy	C2-02	CET	5.0	35	51	0.22	—	137.0	Karlsrud et al. (1993b); and NGI (1988b)
6	Lierstranda	A7-02	CET	5.0	15	29	0.22	—	45.7	Karlsrud et al. (1993b); and NGI (1988a)
7	Lierstranda	A8-02	CET	12.5	22.5	32	0.22	—	45.7	Karlsrud et al. (1993b); and NGI (1988a)
8	Lierstranda	A9-02	CET	20.0	30	31	0.22	—	45.7	Karlsrud et al. (1993b); and NGI (1988a)
9	Lierstranda	A10-02	CET	27.5	37.5	30	0.22	—	45.7	Karlsrud et al. (1993b); and NGI (1988a)
10	Lierstranda	B2-02	OET	5.0	15	52	0.81	0.79	12.3	Karlsrud et al. (1993b); and NGI (1988a)
11	Pentre	A6-02a	CET	25.0	32.5	32	0.22	—	34.2	Karlsrud et al. (1993a, b); NGI (1988c); and Lambson et al. (1993)
12	Pentre	LDP	OEC	15.0	55	44	0.76	0.73	52.5	Gibbs et al. (1993); Cox et al. (1993a, b); and Lambson et al. (1993)
13	Tilbrook	A1	CET	3.0	12.9	61	0.22	—	45.2	Karlsrud et al. (1993a); NGI (1989); and Lambson et al. (1993)
14	Tilbrook	B1	CET	17.5	25.6	59	0.22	—	37.0	Karlsrud et al. (1993a); NGI (1989); and Lambson et al. (1993)
15	Tilbrook	C1	CET	3.0	17.5	59	0.22	—	66.2	Karlsrud et al. (1993a); NGI (1989); and Lambson et al. (1993)
16	Tilbrook	D1	OET	3.0	17.5	73	0.27	0.24	53.1	Karlsrud et al. (1993b); NGI (1989); and Lambson et al. (1993)
17	Tilbrook	LDP-C	OEC	0.0	30	130	0.76	0.70	39.4	Gibbs et al. (1993); Cox et al. (1993a, b); and Lambson et al. (1993)
18	Cowden	A	OEC	0.0	9.2	30	0.46	0.42	20.1	Ridgen et al. (1979); and Gallagher and St. John (1980)
19	Cowden	B	CEC	0.0	9.2	30	0.46	—	20.1	Ridgen et al. (1979); and Gallagher and St. John (1980)
20	AquaticPark	S2-1	OET	57.9	80.5	60	0.76	0.69	29.7	Pelletier and Doyle (1982); and Doyle and Pelletier (1985)
21	Kinnegar	S1	CEC	0.0	6	82	0.25	—	24.0	McCabe and Lehane (2006); and Lehane et al. (2003)
22	Kinnegar	S2	CET	0.0	6	99	0.25	—	24.0	McCabe and Lehane (2006); and Lehane et al. (2003)
23	Kontich	B	OEC	1.5	23.5	21	0.61	0.56	36.1	Heerema (1979); and De Beer et al. (1974)
24	Kansai	T1a	OEC	0.0	32.8	35	1.50	1.46	21.9	Matsumoto et al. (1992); Shibata et al. (1989); and Akai et al. (1991)
25	Kansai	T2	OEC	0.0	48.3	42	1.50	1.46	32.2	Matsumoto et al. (1992); Shibata et al. (1989); and Akai et al. (1991)
26	SintKatelijne	A1	CEC	1.0	7.4	92	0.35	—	18.3	Charue et al. (2001); Huybrechts (2001); and Mengé (2001)
27	SintKatelijne	A4	CEC	1.0	11.6	89	0.35	—	30.3	Charue et al. (2001); Huybrechts (2001); and Mengé (2001)
28	Sandpoint	p	CEC	0.0	45.9	48	0.41	0.38	113.1	Fellenius et al. (2004)
29	WestDelta	LS1	OET	0.0	71.3	116	0.76	0.72	93.6	Bogard and Matlock (1998); Audibert and Hamilton (1998); Ertec (1982); and NGI (1988b)
30	Onsoy2	O1-1	OET	1.4	19.1	78	0.51	0.50	34.8	Karlsrud et al. (2014); and NGI (2013)
31	Cowden2	C2-1	OET	1.0	10	119	0.46	0.43	19.7	Karlsrud et al. (2014); NGI (2013); and Powell and Butcher (2003)
32	Femern	F2-1	OET	0.0	25	34	0.51	0.47	49.2	Karlsrud (2012); and Femern A/S (2014)
33	Stjordal	S2-1	OET	1.0	23.6	50	0.51	0.50	44.5	Karlsrud et al. (2014); and NGI (2013)

Table 2. (*Continued*.)

No.	Site	Test name	Type	Borehole depth (m)	Tip depth (m)	t_{eq} (days)	D (m)	D_i (m)	L/D	Reference
34	Merville	D1	OEC	0.0	9.4	44	0.51	0.48	18.5	Rocher-Lacoste et al. (2004); and Ma and Holeyman (2004)
35	Merville2	B1S1	CEC	4.0	13	57	0.41	—	22.2	Benzaria et al. (2012); and Puech and Benzaria (2013)
36	Merville2	B3S1	CET	4.0	13	62	0.41	—	22.2	Benzaria et al. (2012); and Puech and Benzaria (2013)
37	Klang	TP1A	OEC	0.0	35.5	26	0.25	0.14	142.0	Liew and Kwong (2005)
38	Riau	G1-T1	OEC	0.0	24	73	0.35	0.20	68.6	Liew et al. (2002)
39	Riau	G10-T1	OEC	0.0	30	71	0.35	0.20	85.7	Liew et al. (2002)
40	Riau	G6-T1	OEC	0.0	36	68	0.35	0.20	102.9	Liew et al. (2002)
41	GoldenEars	SC	CEC	0.0	36	120	0.36	—	100.8	Amini et al. (2008)
42	LuluIsland	UBC1	CEC	2.0	14.3	82	0.32	—	38.0	Robertson et al. (1988); and Davies (1987)
43	Borsa	P1 and 2	OET	0.0	50	63	0.41	0.38	123.2	Aas-Jakobsen (2003); and Karlsrud (2012)
45	Quebec	9	CET	2.3	18.1	66	0.32	—	49.5	Fellenius and Samson (1976)
46	Maskinonge	p3	CEC	0.0	23.8	58	0.23	—	103.5	Blanchet et al. (1980)
47	Maskinonge	p4	CEC	0.0	23.8	58	0.22	0.21	108.7	Blanchet et al. (1980)
48	Maskinonge	p5	CEC	0.0	37.5	58	0.23	—	163.0	Blanchet et al. (1980)
49	Goteborg	a	CEC	2.0	18	34	0.24	—	68.1	Bengtsson and Sallfors (1983)

Note: CET = closed ended pile in tension; OET = open ended pile in tension; OEC = open ended pile in compression; and CEC = closed ended pile in compression.

Table 3. Details of pile tests in test database

No.	Site	Test name	Type	Borehole depth (m)	Toe depth (m)	t_{eq} (days)	D (m)	D_i (m)	L/D	Q_m (MN)	Q_c (MN)	Q_m/Q_c	Reference
50	Bayswater	4	OET	1.1	6.2	3	0.17	0.16	30.9	0.038	0.026	1.45	Bittar et al. (2022)
51	CanonsPark	CP5f_L1T	CET	2.1	6	2	0.10		38.2	0.101	0.094	1.07	Bond (1989); and Bond and Jardine (1995)
52	Gloucester	A1	CET	1.0	3	30	0.10		20.0	0.006	0.006	1.05	McQueen et al. (2016); and Hosseini and Rayhani (2015)
53	Gloucester	B1	CET	1.0	3	30	0.10		20.0	0.006	0.006	0.96	McQueen et al. (2016); and Hosseini and Rayhani (2015)
54	Gloucester	C1	OET	1.0	3	30	0.10	0.09	20.0	0.005	0.005	1.08	McQueen et al. (2016); and Hosseini and Rayhani (2015)
55	Haga	2	CET	0.2	5.15	20	0.15		32.4	0.055	0.067	0.82	Karlsrud and Haugen (1985)
56	StAlban	A_3	CET	1.5	7.6	20	0.22		53.9	0.085	0.066	1.29	Roy et al. (1981); and Konrad and Roy (1987)
57	Bothkennar	BK2_L1C	CEC	1.2	6	4	0.10		103.9	0.025	0.017	1.50	Lehane (1992)
58	CanonsPark	AL1C	CEC	3.0	6.5	31	0.17		27.6	0.159	0.255	0.62	Wardle et al. (1992)
59	CanonsPark	BL1C	CEC	2.0	6.5	74	0.17		47.1	0.194	0.272	0.71	Wardle et al. (1992)
60	Cowden	193o	OEC	0.8	9.5	1	0.19	0.18	20.6	0.584	0.368	1.59	Ponniah (1989)
61	Cowden	CW2_L1C	CEC	2.7	6.35	4	0.10		26.5	0.124	0.102	1.22	Lehane (1992)
62	Hangzhou	T2	OEC	0.0	13	17	0.40	0.25	45.1	1.200	0.860	1.40	Kou et al. (2018)
63	Kinnegar	OE1	OEC	2.0	4.04	5	0.17	0.15	36.3	0.012	0.009	1.30	Doherty and Gavin (2011)
64	Pentre	PT3L1T	CET	12.0	17.47	0.7	0.10		32.5	0.075	0.055	1.36	Chow (1996)
65	Pentre	PT5L1T	CET	8.1	18.73	3	0.10		12.0	0.126	0.093	1.35	Chow (1996)
66	Pentre	PT1L1C	CEC	10.5	14.8	0.6	0.10		42.2	0.035	0.045	0.78	Chow (1996)
67	Pentre	PT2L1C	CEC	10.5	19	3	0.10		83.3	0.082	0.092	0.89	Chow (1996)
68	Pentre	PT4L1C	CEC	8.1	14.02	1	0.10		57.6	0.064	0.061	1.06	Chow (1996)
69	Pentre	PT6L1C	CEC	10.2	14	3	0.10		37.3	0.043	0.042	1.03	Chow (1996)
70	Shanghai	159	CEC	0.0	23	3	0.25		92.0	0.620	0.587	1.06	Shanghai Xian Dai (2008)
71	Shanghai	f5	CEC	0.0	22	3	0.25		88.0	0.570	0.709	0.80	Shanghai Xian Dai (2008)
72	Shanghai	p5	CEC	0.0	24	3	0.25		96.0	0.720	0.625	1.15	Shanghai Xian Dai (2008)
73	Shanghai	s73	CEC	0.0	24	3	0.25		96.0	0.915	0.845	1.08	Shanghai Xian Dai (2008)

displacement rate during static load testing ($\dot{s}$), maximum measured axial capacity (Q_m) and measured capacity at a pile head displacement of $0.1D$ ($Q_{m,0.1D}$). The mean pile diameter of 450 mm is significantly smaller than that of a typical pile used offshore. However, laboratory and centrifuge studies (e.g., Potts and Martins 1982; Li and Lehane 2012) have indicated that, unlike piles in sand, scale effects due to the diameter dependence of dilation at the shaft interface do not apply in clays. The database piles were load tested at periods after pile driving (t_{eq}) ranging from 21 to 130 days at stages when their degrees of excess pore pressure dissipation were assessed as being generally greater than 80% (see Lehane et al. 2017).

The measured pile capacity Q_m was taken as the load at a pile head displacement of 10% of the pile diameter ($Q_{m,0.1D}$) or the maximum measured load if this occurred at a lower displacement. The quoted values of Q_m are those arising from the resistance provided by the soil and exclude any contribution to resistance from the weight of piles or soil plugs. The unit shaft capacities assessed from the database test piles assumed that peak frictions (τ_f) operated over the entire pile shaft at the point of overall shaft failure and the formulations for τ_f calibrated from these test data were, therefore, conservative in the few cases in which the long test piles experienced significant progressive softening at a displacement of $0.1D$. Local shaft friction brittleness was generally small, as indicated by the average database $Q_{m,0.1D}/Q_m$ ratio of 0.97 (Table 4).

The base pressure mobilized was lower than the actual $q_{b0.1}$ value in cases when Q_m was greater than $Q_{0.1D}$. However, this effect, as observed in the unified database, was negligible, because

Table 4. Measured and calculated capacities in the unified database

No.	Site	Test name	Type	Q_m (MN)	$Q_{m,0.1D}$ (MN)	s_{max} (mm)	$\dot{s}$ (mm/min)	Q_m/Q_c API-11	Fugro-96	ICP-05	NGI-05	UWA-13	Fugro-10	Eq. (17)
1	Onsøy	A1-02	CET	0.091	0.091	5	0.7	0.85	1.00	0.51	0.90	0.97	0.72	0.74
2	Onsøy	A3-02	CET	0.224	0.224	11	0.6	0.98	1.16	0.63	1.02	1.13	0.89	0.89
3	Onsøy	B1-02	OET	0.427	0.427	8	0.4	1.01	1.06	0.67	1.20	1.29	0.92	0.99
4	Onsøy	C1-02	CET	0.407	0.407	16	1	0.81	1.01	0.54	0.76	0.99	0.81	0.81
5	Onsøy	C2-02	CET	0.487	0.487	13	0.4	0.97	1.21	0.65	0.91	1.18	0.97	0.97
6	Lierstranda	A7-02	CET	0.069	0.069	2	0.5	0.47	0.54	0.23	0.63	0.51	0.36	0.70
7	Lierstranda	A8-02	CET	0.077	0.077	6	0.3	0.35	0.42	0.21	0.59	0.43	0.32	0.64
8	Lierstranda	A9-02	CET	0.1	0.1	15	0.9	0.34	0.41	0.20	0.71	0.43	0.33	0.68
9	Lierstranda	A10-02	CET	0.074	0.074	6	0.5	0.20	0.24	0.12	0.47	0.26	0.20	0.49
10	Lierstranda	B2-02	OET	0.26	0.26	8	0.2	0.45	0.46	0.24	0.64	0.54	0.37	0.75
11	Pentre	A6-02a	CET	0.351	0.351	20	0.4	0.96	1.12	0.60	1.74	1.21	0.81	0.94
12	Pentre	LDP	OEC	6.32	5.8	35	1	0.72	0.81	0.63	1.03	1.35	0.95	1.14
13	Tilbrook	A1	CET	1.246	1.246	15	1	1.29	1.21	1.35	1.10	1.00	1.22	0.98
14	Tilbrook	B1	CET	1.741	1.741	7	1	1.33	1.22	2.00	1.23	1.18	1.18	0.93
15	Tilbrook	C1	CET	2.045	2.045	16	1	1.41	1.34	1.50	1.16	1.05	1.27	0.82
16	Tilbrook	D1	OET	2.039	2.039	9	1	1.10	1.03	1.32	1.07	0.93	1.02	0.74
17	Tilbrook	LDP-C	OEC	16.5	15.2	28	1	1.09	0.99	1.75	1.09	1.10	1.22	1.05
18	Cowden	A	OEC	1.18	1.18	24	1.5	1.46	1.29	1.11	1.53	1.21	1.13	1.09
19	Cowden	B	CEC	1.42	1.39	20	1.5	1.76	1.55	1.06	1.71	1.12	1.36	1.01
20	AquaticPark	S2-1	OET	10.5	10.5	6	—	0.85	0.88	0.84	1.28	1.28	1.02	1.01
21	Kinnegar	S1	CEC	0.073	0.073	15	0.8	0.75	0.71	0.93	0.76	1.12	0.90	1.04
22	Kinnegar	S2	CET	0.065	0.065	20	0.8	0.85	0.80	1.07	0.81	1.37	0.99	1.17
23	Kontich	B	OEC	5.07	4.5	16	1.3	1.43	1.26	2.34	1.42	1.29	1.16	1.06
24	Kansai	T1a	OEC	9.47	10.35	35	—	2.06	1.79	2.13	1.97	2.48	2.21	1.17
25	Kansai	T2	OEC	17.00	16.00	—	—	1.04	1.02	1.59	1.02	1.60	1.25	1.29
26	SintKatelijne	A1	CEC	0.975	0.855	10	(0.2)	2.02	1.70	1.40	1.96	1.12	1.28	1.19
27	SintKatelijne	A4	CEC	1.66	1.41	8	(0.2)	1.81	1.59	1.54	1.76	1.27	1.43	1.33
28	Sandpoint	p	CEC	1.915	1.85	12	(0.2)	0.72	0.81	1.23	0.83	0.95	0.84	1.41
29	WestDelta	LS1	OET	4.29	3.95	24	—	0.98	1.08	0.91	0.97	0.96	1.18	0.81
30	Onsoy2	O1-1	OET	0.519	0.519	12	(0.3)	0.98	1.09	0.76	1.18	1.60	1.11	1.29
31	Cowden2	C2-1	OET	1.02	1.02	26	2	1.54	1.30	1.04	1.58	1.30	1.23	1.02
32	Femern	F2-1	OET	3.12	2.42	15	(0.5)	1.81	1.57	2.95	1.62	1.61	1.43	1.31
33	Stjordal	S2-1	OET	0.64	0.64	30	(0.5)	0.59	0.66	0.48	1.31	1.06	0.66	0.87
34	Merville	D1	OEC	1.165	1.04	6	0.3	1.37	1.15	1.50	1.40	1.30	0.96	0.96
35	Merville2	B1S1	CEC	1.55	1.37	6	0.3	1.59	1.38	1.17	1.56	1.02	1.14	0.79
36	Merville2	B3S1	CET	1.4	1.13	6	0.3	1.88	1.56	1.49	1.80	1.23	1.38	0.92
37	Klang	TP1A	OEC	0.635	0.635	20	(0.5)	0.80	0.92	1.06	0.70	1.09	0.82	0.82
38	Riau	G1-T1	OEC	0.425	0.425	30	(0.5)	0.97	1.00	1.64	0.85	1.00	0.84	0.81
39	Riau	G10-T1	OEC	0.5	0.5	30	(0.5)	0.74	0.78	1.17	0.65	0.83	0.70	0.68
40	Riau	G6-T1	OEC	0.7	0.7	30	(0.5)	0.72	0.77	1.20	0.63	0.81	0.67	0.66
41	GoldenEars	SC	CEC	2.8	2.8	20	(0.1)	1.39	1.43	1.86	1.25	1.48	1.35	1.26
42	LuluIsland	UBC1	CEC	0.225	0.225	15	(0.3)	0.58	0.62	0.41	0.68	1.08	0.82	0.83
43	Borsa	P1&2	OET	1.615	1.615	40	1.4	0.48	0.56	0.37	0.85	0.80	0.60	1.38
45	Quebec	9	CET	0.426	0.37	15	(0.2)	0.84	0.80	1.30	0.79	0.89	0.77	0.91
46	Maskinonge	p3	CEC	0.61	0.53	3	0.4	1.37	1.60	1.89	1.27	1.69	1.32	1.48
47	Maskinonge	p4	CEC	0.4	0.4	6	0.4	0.99	1.17	1.38	0.92	1.24	0.96	1.03
48	Maskinonge	p5	CEC	0.88	0.785	17	0.4	0.95	1.18	1.64	0.85	1.22	0.97	1.07
49	Goteborg	a	CEC	0.23	0.23	5	1	0.86	0.91	1.27	0.84	0.99	0.79	1.00

Note: UWA = University of Western Australia.

J. Geotech. Geoenviron. Eng., 2022, 148(9): 04022069

the base resistance typically represented only about 10% of compression pile capacity, and gains in base resistance between the displacement at maximum load (typically 5% of the diameter for the cases with $Q_m > Q_{0.1D}$) and $0.1D$ were low.

The creep rate $(\dot{s})$ recorded at maximum capacity for the piles in the unified database varied in almost all cases between values of 0.2 and 1.0 mm/min. Creep rates are shown bracketed in Table 4 for cases in which they were not documented explicitly and needed to be estimated from the reported load test durations, allowing for typical increases in creep rate as loading progresses. Load tests investigating the influence of displacement rate on capacity in high plasticity Bothkennar clay (Lehane and Jardine 1994a) have shown that capacities differed by less than 5% when $\dot{s}$ varied between 0.05 mm/min and 3 mm/min but that viscous effects became more prominent at higher velocities (increasing shaft resistance by about 10% per log cycle increase in $\dot{s}$). The values of Q_m in the database may, therefore, be presumed to be insensitive to the range of creep rates that occurred in the load tests.

The soil properties in both the unified and test databases are summarized by presenting the median values in clay strata of the CPT consistency index I_c, CPT friction ratio F_r, and plasticity index I_p along the embedded lengths of the piles. Median values are employed because they provide more representative measures when there is significant layering at a given test site. They are plotted on the SBT chart in Fig. 6 and on the plasticity chart in Fig. 7. Fig. 6 shows that the majority of the 31 clay sites fall within Zone 3 (silty clay to clay) and Zone 4 (clayey silt to silty clay) and are either lightly overconsolidated with normalized cone resistances

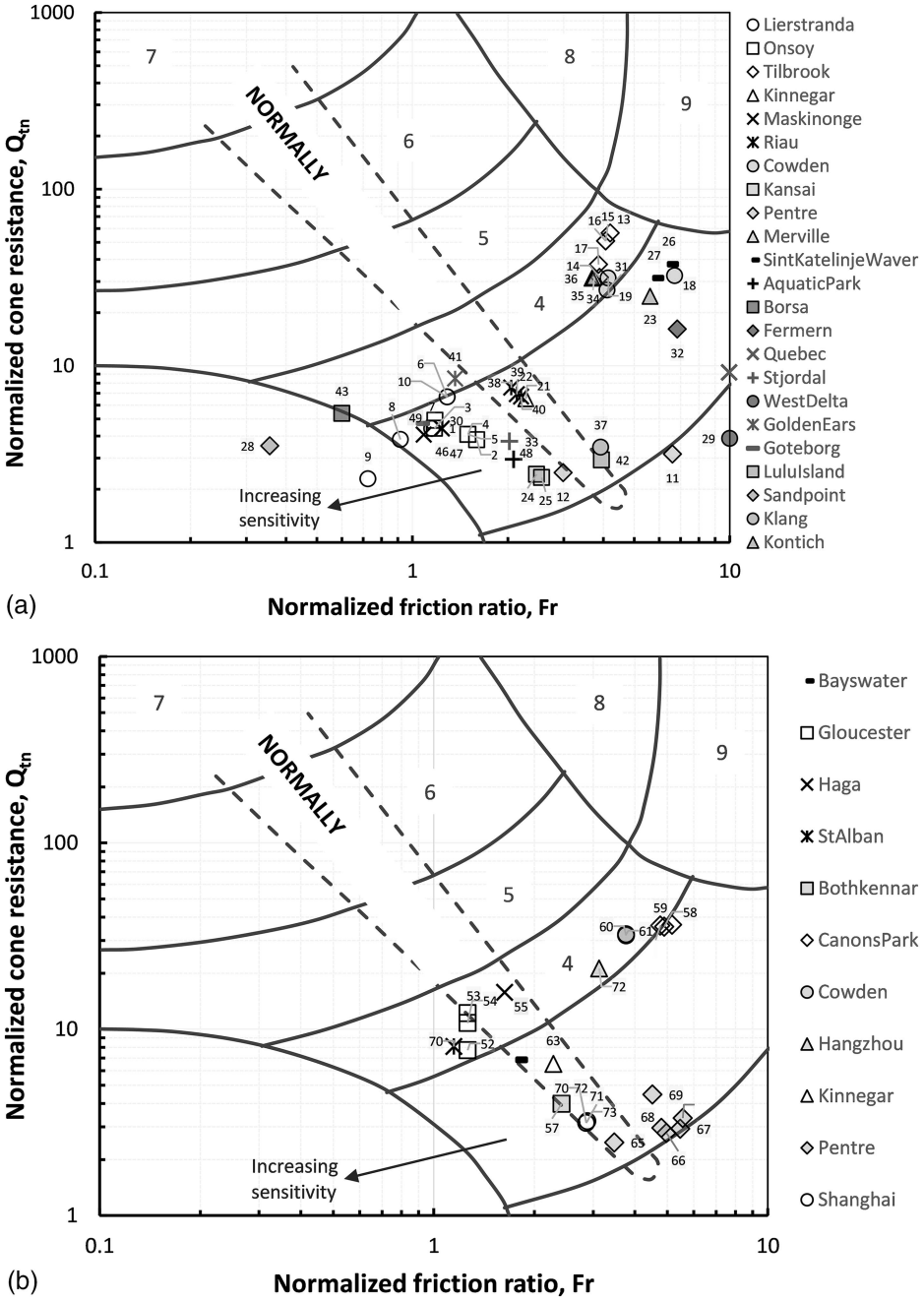

Fig. 6. SBT chart using median values at site of pile tests in the: (a) unified database; and (b) test database. Pile numbers refer to the pile numbers in Tables 2 and 3.

J. Geotech. Geoenviron. Eng., 2022, 148(9): 04022069

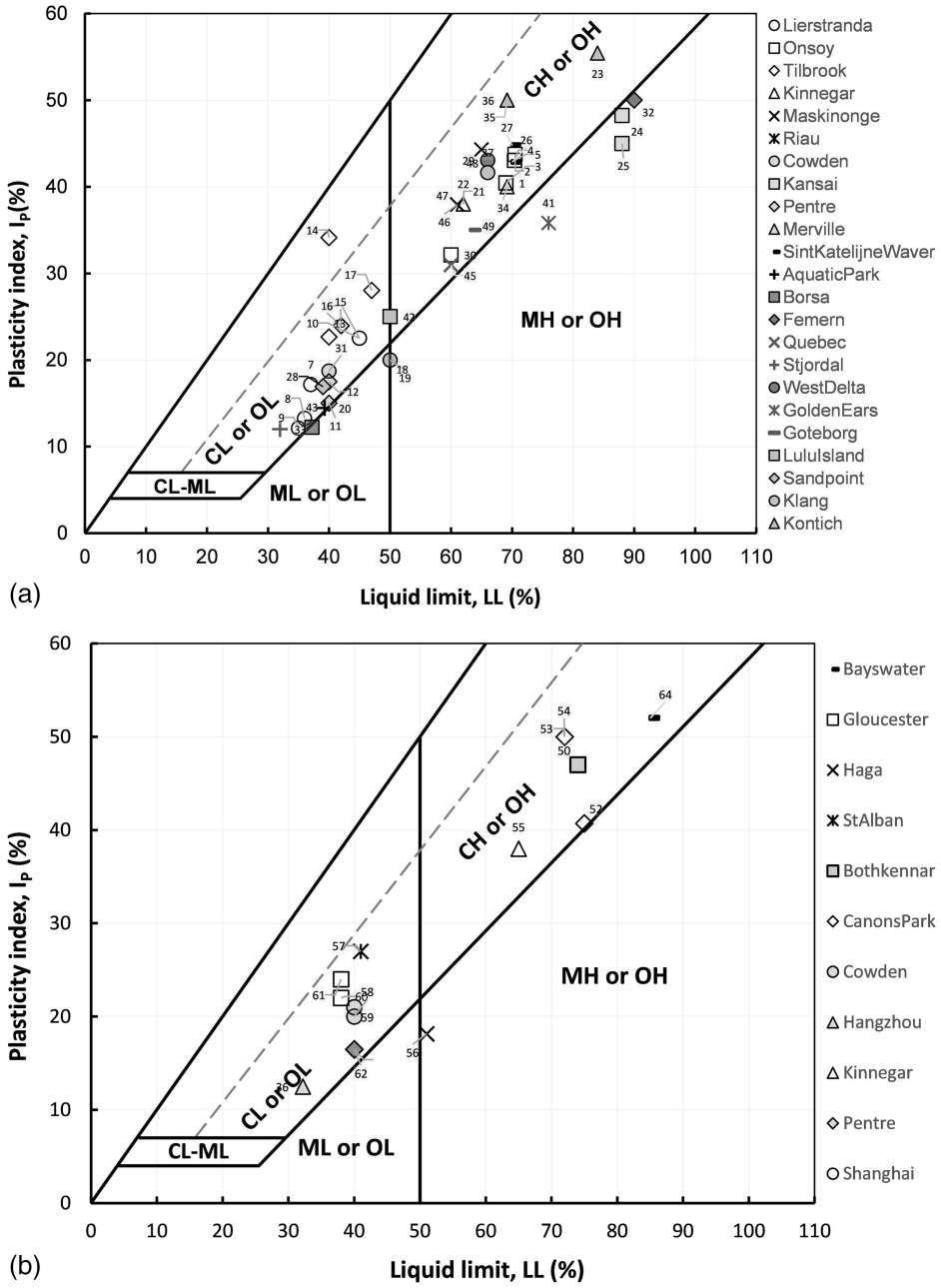

Fig. 7. Plasticity chart using median values at sites of pile tests in the: (a) unified database; and (b) test database. Pile numbers refer to the pile numbers in Tables 2 and 3.

(Q_{tn}) of 5 ± 3 or have high OCRs with $Q_{tn} = 35 \pm 10$. Two clays (Pentre and West Delta) lie in Zone 2 (organic soils and clay), while three soils, namely Lierstranda, Sandpoint, and Borsa clays, lie close to or within Zone 1 (sensitive clays).

Fig. 7 shows that the database comprises a large and uniform spread in I_p and liquid limit values, in which all soils plot above (or just below) the A-line. It is interesting that, while the four clays classified in Zone 1 are of low plasticity ($I_p < 20\%$), the Pentre clay, with a comparably low plasticity index ($I_p = 16\%$), plots in Zone 2 and has a measured sensitivity (S_t) of only of 1.5 (Chow 1997).

Optimization Analyses

The instrumented pile test records showed that the dominant parameters controlling local shaft friction (τ_f) were the CPT resistance (q_t) and the length effect, as described by the h/D term. Initial calculations showed that use of the distance h rather that the normalized value (h/D) provided less satisfactory fits to the data. Additional terms were also examined using the following two formats and assuming that the dependence of these terms could be represented as power functions (where C_1 and C_2 are constants)

$$\tau_f = C_1 \times q_t^a \times \sigma_v'^b \times (h/D)^{-c} \times A_{re}^d \times F_r^e \times I_c^f \times I_p^g \times f_D \times F_{st} \quad (14)$$

$$\tau_f = C_2 \times q_t^a \times \sigma_v'^b \times (h/D^*)^{-c} \times F_r^e \times I_c^f \times I_p^g \times f_D \times F_{st} \quad (15)$$

where parameters a, b, c, d, e, f, and g = fitting parameters; and a minimum h/D^* or h/D value was nominally taken equal to 1.0. Capacities were calculated for various combinations of these

parameters using Eq. (13) to determine the base resistance of compression piles and assuming initially that τ_f could be represented as a product of the power functions. Eqs. (14) and (15) were used for calculation of τ_f in clay strata with $I_c > 2.5$, while the recommendations of the new ISO 19901-4 CPT sand method (Lehane et al. 2020) were applied directly in sand and silty sand layers with $I_c < 2.05$. In (occasional) silt layers in the database with I_c in the range between 2.05 and 2.5, the sand method was employed using the equivalent clean sand q_t value ($q_{t,\text{sand}}$), derived using the following relationship, which is equivalent to the proposal of Robertson and Wride (1998) but adapted to a simplified format and modified to give a correction factor of unity at $I_c = 2.05$

$$q_{t,\text{sand}} = [3.93I_c^2 - 14.78I_c + 14.78]q_t \quad \text{for } 2.05 < I_c < 2.5 \quad (16)$$

A spreadsheet-based optimization scheme was set up using the generalized reduced gradient approach (Baker 2011) to determine the combination of fitting parameters that minimized the coefficient of variation of the ratios of measured to calculated capacities (Q_m/Q_c) and gave an average Q_m/Q_c ratio of unity for all 49 piles in the unified database. The spreadsheet results were verified independently using a Python code version 3.8.0 that used the sequential least-squares programming (SLSQP) algorithm.

A variety of different constraints were applied to the variables to ensure that (1) the local minimum determined was a feasible solution; (2) differences between calculated distributions of τ_f and those reported in available case histories were small (e.g., Fig. 8); and (3) the expression for τ_f was consistent with trends indicated in instrumented pile tests (Fig. 5). Preliminary analyses examined trends of Q_m/Q_c values with respect to individual terms in Eqs. (14) and (15) as well combinations of these terms (e.g., Fig. 9). The analyses confirmed the general versatility of using power functions to assess the relative impact of the terms and combinations of these terms.

Each Q_m/Q_c value was weighted following a procedure described in Lehane et al. (2017) to deduce a weighted coefficient of variation (COV_w) for Q_m/Q_c ratios. Lower weightings were applied to multiple piles at the same site, and the weightings also varied with the quality ratings assigned to each test pile by the team of experts responsible for compiling the database (Lehane et al. 2017). Despite these procedures, the results of the analyses showed negligible differences between the statistics for weighted and unweighted coefficients of variation.

The analyses revealed the following key findings:

1. The lowest COV_w values were deduced when the exponent for q_t was unity and the exponent for σ'_v [see Eqs. (14) and (15)] was close to zero. Consequently, unlike the α design method, such as that recommended in API (2011), the analyses did not indicate a dependence of τ_f on q_t/σ'_v, which varied approximately with the undrained strength ratio and OCR. This characteristic was in keeping with the trends inferred from the instrumented pile tests in Fig. 5.
2. For any combination of the fitting parameters, Q_m/Q_c ratios determined in three of the Zone 1 clays (in particular, the Lierstranda clay) were significantly overpredicted when F_{st} was assumed equal to unity. Consequently, optimization focused on pile tests in clays outside of Zone 1 and then revisited the tests in Zone 1 to deduce recommendations for F_{st}.
3. Inclusion of the F_r and I_c terms in the formulation had no beneficial effect on the goodness-of-fit with the pile load tests in the unified database; that is, optimized e and f parameters were effectively zero, and the same best-estimate formulation was applicable to clays in Zones 2, 3, and 4 of the SBT chart.
4. The optimized exponent to I_p was close to zero, indicating no effect of plasticity index on the best-fit τ_f formulation. This finding contrasted with the strong dependence on I_p incorporated in the α method of Karlsrud et al. (2005).
5. The minimum COV_w values achieved using the function forms in Eqs. (14) and (15) were identical, and, therefore, Eq. (15),

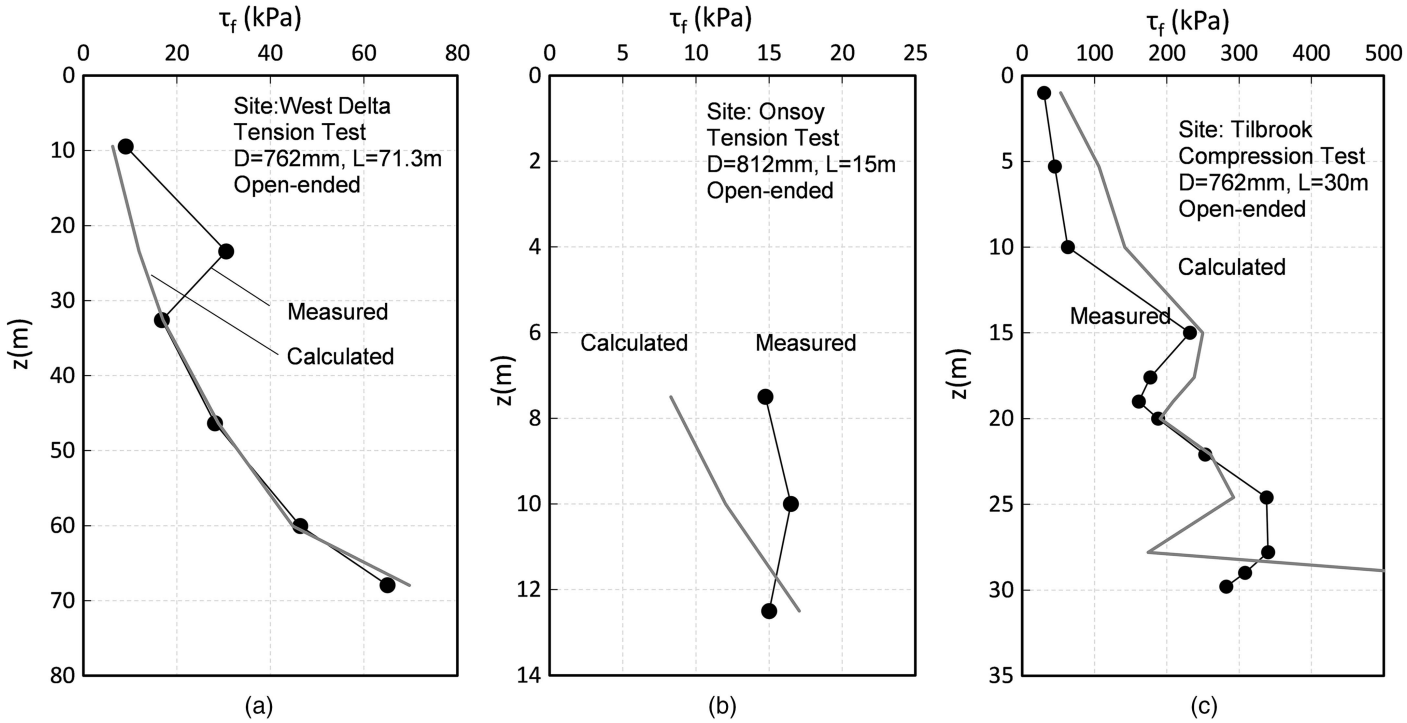

Fig. 8. Comparison of measured and calculated ultimate shaft friction profiles for three test piles in the unified database.

J. Geotech. Geoenviron. Eng., 2022, 148(9): 04022069

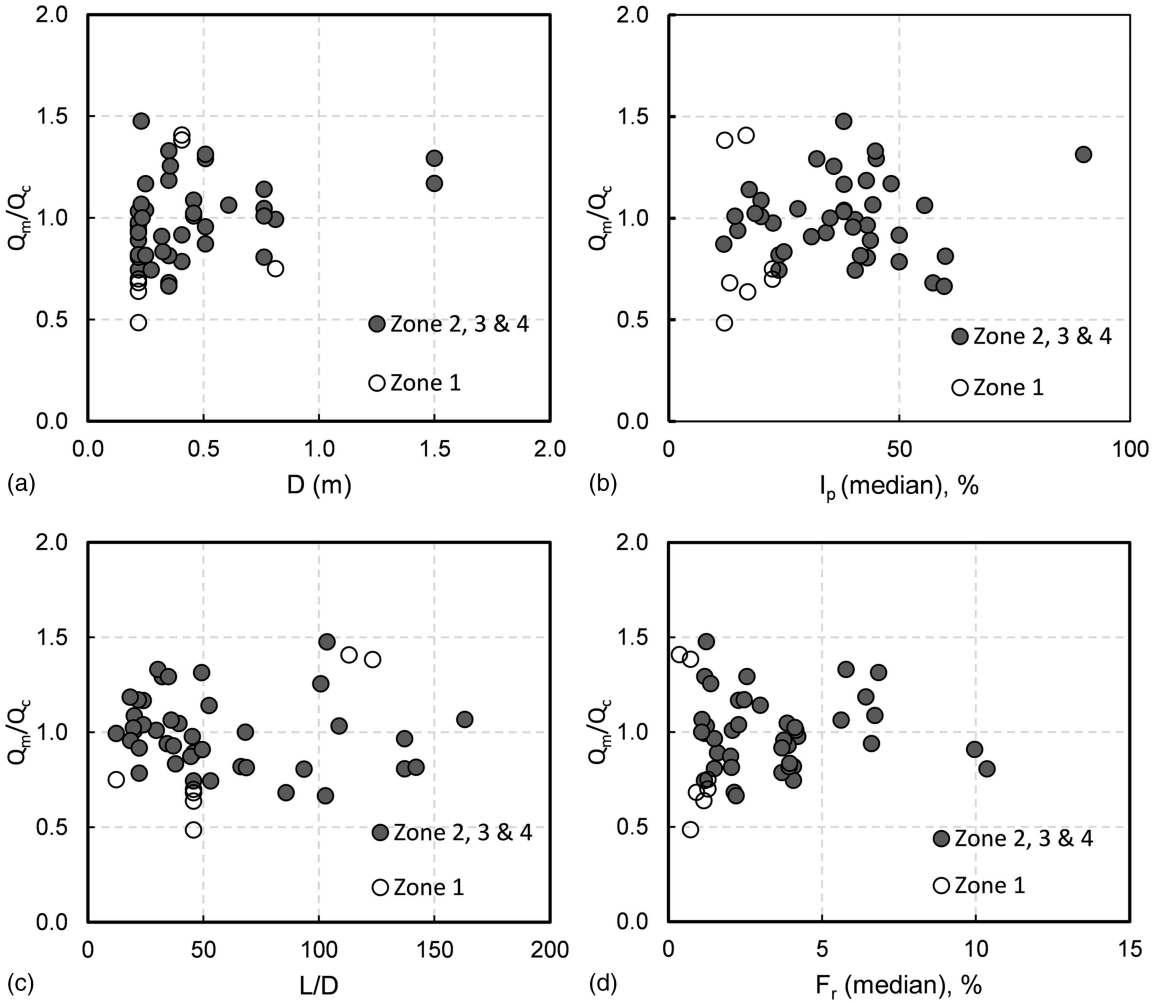

Fig. 9. Variations of ratio Q_m/Q_c with D, L/D, I_p, and F_r for unified database, determined using Eq. (17).

which uses the h/D^* term, was adopted for simplicity. Eq. (15) reduces to Eq. (14) if the exponent d of the effective ratio A_{re} equals $-c/2$. The statistical analyses predicted d values that were close to $-c/2$, hence justifying use of Eq. (15).

6. Similar COV_w values were obtained when f_D was varied between 0.85 and 1.15, indicating that f_D can be set equal to unity in line with the average parameter deduced from field tests discussed previously.
7. COV_w values showed marginal differences for c varying between 0.15 and 0.3 (where c is the exponent for h/D^*). A c value of 0.25 was selected, because it provided a slightly improved fit to the ultimate shear stress profiles recorded on test piles, especially large diameter pipe piles.

The initial, convenient assumption that the contribution of F_r, I_c, and I_p to τ_f could be represented in the optimization analysis as the product of power functions of these terms was warranted because of the absence of any individual or combined contribution to the best-fit formulation. Consideration of the product of the q_t and σ'_v terms enabled an indirect check on the influence of undrained strength ratio, while the inclusion in the formulation of the product of q_t with h/D or h/D^* terms was consistent with the trend shown in Fig. 5. Therefore, despite the wide-ranging investigation into potentially influential factors, the statistical analyses indicated that the following simple correlation for peak friction in tension and compression provided a best fit to the unified database

$$\tau_f = 0.07 F_{st} q_t \text{Max}[1, (h/D^*)]^{-0.25}$$

where $F_{st} = 1$ for clays in Zones 2, 3, and 4, and

$$F_{st} = 0.5 \pm 0.2 \quad \text{for Zone 1 clays} \tag{17}$$

It is encouraging that Eq. (17) is almost identical to Eq. (7), which was deduced independently from instrumented pile test data. The predictive performance of Eq. (17) for the unified database was examined in terms of ratios of measured to calculated capacities (Q_m/Q_c) in Tables 4 and 5, in which it was compared with predictions for the piles in the unified database using six other published formulations for τ_f ; further details are provided in Lehane et al. (2017). The statistics for the Q_m/Q_c values provided in Table 4 are given in Table 5, which also lists the parameters employed in each of the τ_f formulations (noting that the contributions of base resistance to the capacities were very small). It is evident that the mean Q_m/Q_c value for each formulation was close to unity but that the spread in predictions for Eq. (17), as measured by the COV for Q_m/Q_c (and, hence, its predictive reliability), is far less than the spread of the six other methods, indicating a significantly higher level of reliability. The COV values for Q_m/Q_c for the other methods were in the range of 0.3 to 0.6, which was consistent with the range quoted by Paikowsky et al. (2004) and Dithinde et al. (2011) for predictive methods in general.

J. Geotech. Geoenviron. Eng., 2022, 148(9): 04022069

Table 5. Statistics for Q_m/Q_c for the unified database for different τ_f formulations

Method	Correlation type with τ_f	Mean Q_m/Q_c	COV for Q_m/Q_c	Reference
API	s_u and s_u/σ'_v	1.05	0.43	API (2011)
Fugro-96	s_u, h/D, and s_u/σ'_v	1.04	0.35	Kolk and van der Velde (1996)
ICP-05	OCR, σ'_v, h/D^*, δ, S_t, and σ'_v	1.12	0.55[a]	Jardine et al. (2005)
NGI-05	s_u, s_u/σ'_v, I_p, and σ'_v	1.1	0.36	Karlsrud et al. (2005)
UWA-13	q_t and h/D^*	1.12	0.33	Lehane et al. (2013)
Fugro-10	q_{net}, h, and q_{net}/σ'_v	0.98	0.37	Van Dijk and Kolk (2010)
Eq. (17)	q_t, h/D^* and S_t	0.99	0.23	This paper

[a]This high COV arises because of uncertainty related to the parameters required by this approach for many of the database piles.

The best-fit F_{st} values were 0.3 in Lierstranda clay and 0.7 in Borsa and Sandpoint clays. It is therefore evident that the analyses did not lead to a unique F_{st} value for Zone 1 clays; as a result, there is additional uncertainty related to use of the proposed F_{st} value of 0.5 for these clays. Consequently, pile capacities in Zone 1 soils need to be assessed with particular care and should ideally rely on local experience and pile testing. In this regard, it is important to note that the measurement of CPT friction sleeve stress is prone to error and may lead to misclassification of the soil type. Additional investigations to assist in a material's classification are recommended if the CPT data plot close to the Zone 1 boundary. It is also noteworthy that the COV for Q_m/Q_c for Eq. (17), excluding Zone 1 pile tests, reduce to a value of 0.19 with a mean Q_m/Q_c of unity; COV values showed comparable reductions for the other methods included in Table 5 when Zone 1 pile tests were excluded.

The peak shear stress profiles calculated using Eq. (17) are compared in Fig. 8 with profiles measured by three of the larger diameter pipe piles in the unified database. The profile for the very long pile in the soft clay at West Delta is well predicted, while predictions in the low-OCR clay at Onsøy and high-OCR clay at Tilbrook provide less precise matches to the measured distributions. While such differences may be partly attributed to errors in the friction inferred from measured axial load distributions and to difficulties in separating end bearing and external friction for the compression pile at Tilbrook, the comparisons serve to highlight the approximate and empirical nature of Eq. (17).

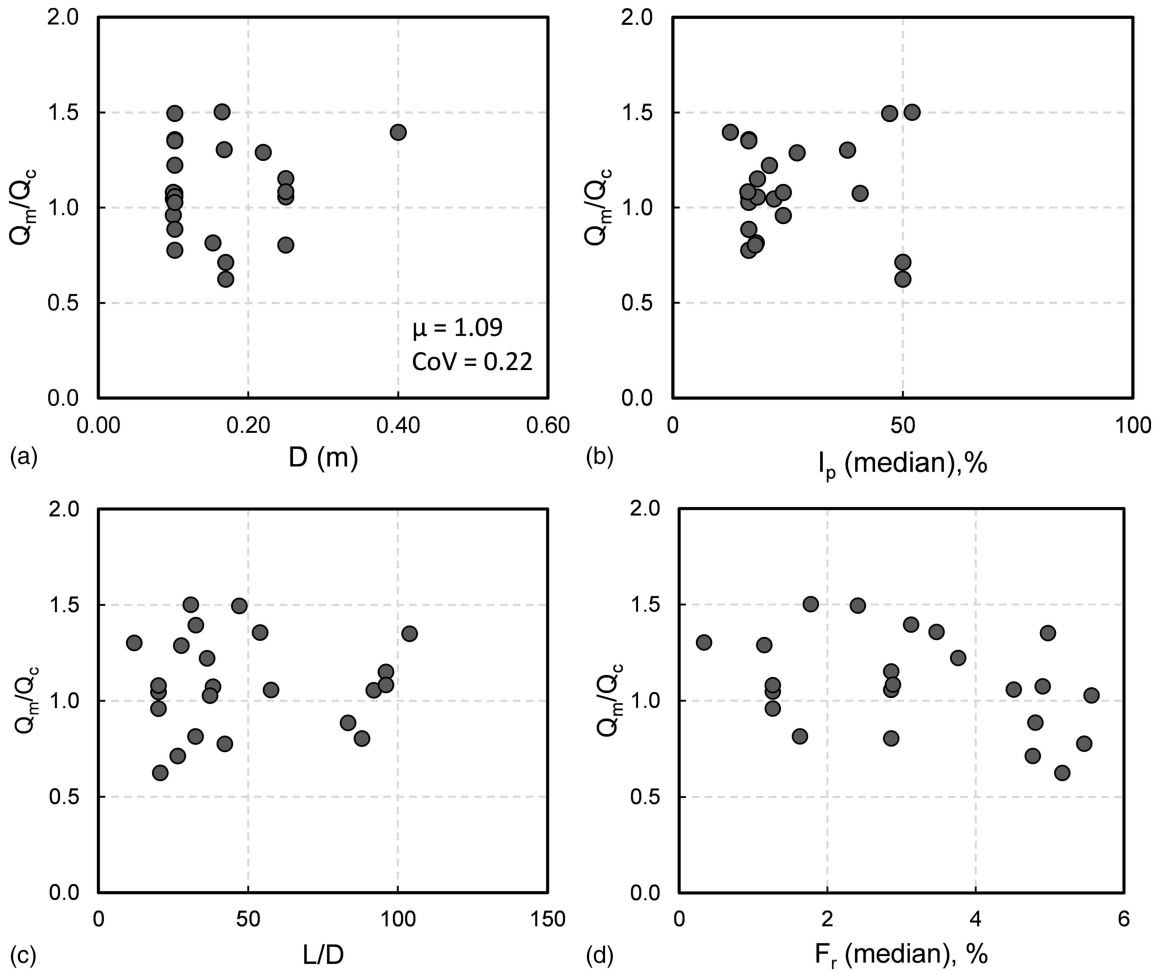

Fig. 10. Variations of Q_m/Q_c with D, L/D, I_p, *and* F_r for test database, determined using Eq. (17).

The optimization analyses included a constraint to minimize the bias of Q_m/Q_c with respect to additional pile and soil parameters. To examine such bias, these ratios were plotted for the unified database in Fig. 9 against pile diameter, pile slenderness ratio (L/D), median friction ratio (F_r), and the median plasticity index (I_p). Best-fit regression lines for each set of data indicate no clear dependence of Q_m/Q_c on L/D, F_r, and I_p. The slight apparent trend seen in Fig. 9(a) to overestimate pile capacity (i.e., $Q_m/Q_c > 1$) as the diameter increases arises because of the two 1.5-m-diameter piles at Kansai (Matsumoto et al. 1992). These piles were driven into a clay deposit that included significant sand layers and, as such, their quality rating and hence weighting applied to the overall statistics was relatively low in the analyses.

Eq. (17) provides an expression for peak shaft friction that should be used in a load transfer analysis to determine pile response under load. A load transfer analysis is also required to determine the capacity of long slender piles using t-z springs that include the postpeak softening branches recommended by API (2011) or take account of other site-specific softening data. Such analyses were performed for the unified database piles using the t-z curves documented in API (2011) and the average recommended softening coefficient of 0.8. The analyses had little effect on the evaluated Q_m/Q_c ratios for piles with $L/D < 50$ but increased the ratios to values in excess of 0.75 for all piles with $L/D > 50$; that is, potential nonconservatism was reduced.

Postconsolidation gains in shaft capacity are referred to as aging (e.g., Doherty and Gavin 2013). Eq. (17) does not incorporate an aging enhancement factor and provides a means of estimating shaft friction when the degree of excess pore pressure dissipation after driving is more than 80%. According to Teh and Houlsby (1991) and Randolph (2003), in a typical clay, achieving this level of dissipation at the shaft of a 2-m-diameter offshore pipe pile with a wall thickness of 40 mm may take 6 months or longer, while 80% dissipation for a 250-mm-square precast concrete pile would generally be complete in 3 to 4 weeks. It should also be noted that the development of dilative local shaft effective stress paths and other effects at low levels of equalization may compensate partially for low radial effective stresses, with the consequence that partially equalized shaft frictions are often higher than anticipated from the degree of pore pressure dissipation (see for example, Lehane and Jardine 1994a; Basu et al. 2014; Bittar et al. 2022).

The test database, summarized in Table 3, was used to obtain an independent check of the best-fit formulation [Eq. (17)] and involved an additional eight clay types (all lying in Zones 3 and 4 on the SBT chart). Although these piles were generally smaller in diameter and shorter than those in the unified database, it was found that Eq. (17) predicted the capacity relatively well, with an average Q_m/Q_c value of 1.09 (i.e., slightly conservative in terms of predicted capacity) and a coefficient of variation for Q_m/Q_c of 0.22. Bias charts for the predictions for the test database are provided in Fig. 10 and demonstrate no obvious dependence of Q_m/Q_c on D, L/D, or I_p but do display a tendency for Q_m/Q_c to decrease slightly with F_r. However, this trend was not evident in the analysis of the unified database, which comprises about three times more tests.

The statistics for the test database are consistent with those of the unified database and provide additional evidence in support of the general applicability of Eq. (17). It is of note that the outlier Q_m/Q_c values in the test database occurred for the piles in Bothkennar and London clays and averaged 1.5 and 0.67, respectively. These relatively large deviations from the average, which were also evident in Fig. 5, partially reflected the relatively high δ value of 29° in Bothkennar clay and relatively low δ value of 13° in London clay and suggest that improvements in predictive performance in future correlations may be achieved if δ values are measured and documented reliably for new test piles. The variability of Q_m/Q_c in Figs. 9 and 10 is a simple consequence of the limitations of the CPT-based formulation and variability in pile load test results.

Conclusions

This paper presented the development of a new CPT-based method for assessment of the axial capacity of driven piles in clay. Eq. (12) provides an expression deduced for the ultimate end-bearing capacity (defined at a displacement of 10% of the pile diameter), while the expression for peak local shaft friction is given in Eq. (17); these equations at slow rates of loading (typical of static load tests) after equalization of excess pore pressures. The equations are consistent with findings from field research and numerical analyses and were calibrated using the unified database of pile load tests published in Lehane et al. (2017). The method is a significant improvement on popular existing methods and was shown to provide good predictions for both the unified database and an additional test database that was compiled to enable an independent check of the method. Measured ultimate shaft friction distributions were also seen to be reasonably well estimated. While providing generally good predictions for the particular database used for its calibration, its empirical formulation is recognized, and designers should exercise due caution with the approach, especially when considering sensitive clays.

Data Availability Statement

All data and models used during the study appear in the published article.

Acknowledgments

The authors gratefully acknowledge the funding and support provided under a JIP funded by Aramco, Equinor, Lundin, Ørsted, Oil and natural Gas Corporation Ltd. (ONGC), BP, Total, ExxonMobil, Energie Baden-Württemberg AG (EnBW), Electricitie de France (EDF), and Scottish and Southern Energy Renewables (SSER). The significant contributions of Dr. Jit Kheng Lim to database compilation is also highly appreciated, as are the technical contributions of the JIP steering committee members to the development of the method.

Notation

The following symbols are used in this paper:

A_{re} = effective area ratio (ratio of soil displaced by pipe pile to displacement by closed-ended pile);
COV_w = weighted coefficient of variation;
c = exponent to h/D and h/D^*;
D = pile diameter;
D_{eq} = diameter of an equivalent closed-ended pile that induces the same soil displacement during installation as a pipe pile;
D_i = inner pile diameter (of pipe pile);
D^* = D_{eq} value for full coring pipe pile or D for closed-ended pile;
d_{CPT} = diameter of a standard cone penetrometer;

F_r = CPT friction ratio;
F_{st} = sensitivity coefficient;
f_D = load direction coefficient for shaft friction;
f_L = loading coefficient ($\sigma'_{rf}/\sigma'_{rc}$);
h = height of given point on the shaft above the pile base;
I_c = CPT soil consistency index;
I_p = plasticity index;
L = pile length;
Q_c = calculated pile capacity;
Q_m = measured pile capacity (defined at $s = 0.1D$ if not attained at lower s);
$Q_{m,0.1D}$ = measured pile head load at $s = 0.1D$;
Q_{tn} = normalized cone resistance (see Robertson 2009);
$q_{b0.1}$ = end-bearing stress at a pile base displacement of $D/10$;
q_c = cone resistance;
q_t = cone resistance corrected for pore pressure at filter;
q_{net} = net cone resistance = $q_t - \sigma_{v0}$;
$q_{t,\text{sand}}$ = q_t measured at drained rate of penetration in silt;
s = pile head displacement in load test;
s_u^{UU} = triaxial compression UU shear strength;
$\dot{s}$ = maximum pile displacement rate in static load test;
$s_{\max}$ = pile head displacement at Q_m;
t_{eq} = time between installation and load testing;
u_0 = ambient (hydrostatic) pore pressure;
α = adhesion factor (τ_f/s_u^{UU});
Δu_i = excess pore pressure at pile shaft during installation;
δ = clay-pile interface friction angle;
μ = mean value of Q_m/Q_c;
σ_{rc}, σ'_{rc} = radial total and effective stress, respectively, after equalization of pore pressure;
σ_{ri}, σ'_{ri} = radial total and effective stress, respectively, operating during installation;
σ'_{rf} = radial effective stress at peak shear stress in load test;
σ'_{v0} = in situ vertical effective stress; and
τ_f = peak shear stress.

References

Aas-Jakobsen. 2003. *Borsa site investigation*. Rep. No. 7618-K030-G-005. Oslo, Norway: Aas-Jakobsen.

Akai, K., K. Nakaseko, T. Matsui, M. Kamon, Y. Tanaka, and S. Suwa. 1991. "Geotechnical properties of marine clays in Osaka Bay." In Vol. 1 of *Proc., Geo-Coast '91*, 5–11. Tokyo: Coastal Development Institute of Technology.

Almeida, M. S., F. A. Danziger, and T. Lunne. 1996. "Use of the piezocone test to predict the axial capacity of driven and jacked piles in clay." *Can. Geotech. J.* 33 (1): 23–41. https://doi.org/10.1139/t96-022.

Amini, A., B. H. Fellenius, M. Sabbagh, E. Naesgaard, and M. Buehler. 2008. "Pile loading tests at Golden Ears Bridge." In *Proc., 61st Canadian Geotechnical Conf.*, 8. Edmonton, Canada: Canadian Geotechnical Society.

API (American Petroleum Institute). 2011. "ANSI/API RP 2GEO: Geotechnical and foundation design considerations. ISO 19901-4:2003 (modified)." In *Petroleum and natural gas industries—Specific requirements for offshore structures, part 4—Geotechnical and foundation design considerations*. 1st ed. Washington, DC: API Publishing Services.

Audibert, J. M. E., and T. K. Hamilton. 1998. "West Delta 58A Site Selection and Characterization." In Vol. 1 of *Proc., Offshore Technology Conf.*, 415–431. Houston: Offshore Technology Conference.

Azzouz, A. S., M. M. Baligh, and A. J. Whittle. 1990. "Shaft resistance of piles in clay." *J. Geotech. Eng.* 116 (2): 205–221. https://doi.org/10.1061/(ASCE)0733-9410(1990)116:2(205).

Azzouz, A. S., and M. J. Morrison. 1988. "Field measurements on model pile in two clay deposits." *J. Geotech. Eng.* 114 (1): 104–121. https://doi.org/10.1061/(ASCE)0733-9410(1988)114:1(104).

Baker, K. R. 2011. *Optimization modelling with spreadsheets*. New York: Wiley.

Basu, P., M. Prezzi, R. Salgado, and T. Chakraborty. 2014. "Shaft resistance and setup factors for piles jacked in clay." *J. Geotech. Geoenviron. Eng.* 140 (3): 57–73. https://doi.org/10.1061/(ASCE)GT.1943-5606.0001018.

Bengtsson, P.-E., and G. Sällfors. 1983. "Floating piles in soft, highly plastic clays." *Can. Geotech. J.* 20 (1): 159–168. https://doi.org/10.1139/t83-014.

Benzaria, O., A. Puech, and A. Kouby. 2012. "Cyclic axial load tests on driven piles in overconsolidated clay." In *Offshore site investigation and geotechnics 2012: Integrated technologies—Present and future*, 307–314. London: The Society for Underwater Technology.

Bittar, E., B. Huang, B. M. Lehane, and P. Watson. 2022. "Pile ageing to support life extension of offshore platforms." In *Proc., 20th Int. Conf. Soil Mechanics Geotechnology Engineering*. Sydney, Australia: Australian Geomechanics Society.

Blanchet, R., F. Tavenas, and R. Garneau. 1980. "Behaviour of friction piles in soft sensitive clays." *Can. Geotech. J.* 17 (2): 203–224. https://doi.org/10.1139/t80-023.

Bogard, D., and H. Matlock. 1998. "Static and cyclic load testing of a 30-inch-diameter pile over a 2.5-year period." In *Proc., Offshore Technology Conf.* Richardson, TX: Offshore Technology Conference.

Bond, A. J. 1989. "Behaviour of displacement piles in overconsolidated clays." Ph.D. thesis, Dept. of Civil Engineering, Imperial College London (Univ. of London).

Bond, A. J., and R. J. Jardine. 1991. "Effects of installing displacement piles in high OCR clay." *Géotechnique* 41 (3): 341–363. https://doi.org/10.1680/geot.1991.41.3.341.

Bustamante, M., and L. Gianeselli. 1982. "Pile bearing capacity prediction by means of static penetrometer CPT." In *Proc., 2nd European Symp. on Penetration Testing*, 493–500. Boca Raton, FL: CRC Press. https://doi.org/10.1201/9780203743959.

Charue, N., N. Huybrechts, and A. Holeyman. 2001. "Prediction and verification of a precast concrete pile driven in Boom clay." In *Proc., 15th Int. Conf. of Soil Mechanics in Geotechnical Engineering*, 863–866. Boca Raton, FL: CRC Press.

Chin, C. T. 1986. "Open-ended pile penetration in saturated clays." Ph.D. thesis, Dept. of Civil Engineering, Massachusetts Institute of Technology.

Chow, F. 1997. "Investigations into the behaviour of displacement piles for offshore foundations." Ph.D. thesis, Dept. of Civil Engineering, Imperial College London (Univ. of London).

Coop, M. R., and C. P. Wroth. 1989. "Field studies of an instrumented model pile in clay." *Géotechnique* 39 (4): 679–696. https://doi.org/10.1680/geot.1989.39.4.679.

Cox, W. R., K. Cameron, and J. Clarke. 1993a. "Static and cyclic axial load tests on two 762 mm diameter pipe piles in clays." In *Proc., Conf. Large-Scale Pile Tests in Clay*, 268–284. London: Thomas Telford.

Cox, W. R., I. J. Solomon, and K. Cameron. 1993b. "Instrumentation and calibration of two 762mm diameter pipe piles for axial load tests in clays." In *Proc., Conf. Large-Scale Pile Tests in Clay*, 217–236. London: Thomas Telford.

Davies, M. P. 1987. "Predicting axially and laterally loaded pile behaviour using in-situ testing methods." M.Sc. dissertation, Dept. of Civil Engineering, Univ. of British Columbia.

De Beer, E. E., E. Lousberg, M. Wallays, R. Carpentier, J. De Jaeger, and J. Paquay. 1974. "Scale effects in results of penetration tests performed in stiff clays." In *Proc., European Conf. on Penetration Testing*, 105–114. Boca Raton, FL: CRC Press.

Dithinde, M., K. K. Phoon, M. De Wet, and J. V. Retief. 2011. "Characterization of model uncertainty in the static pile design formula." *J. Geotech. Geoenviron. Eng.* 137 (1): 70–85. https://doi.org/10.1061/(ASCE)GT.1943-5606.0000401.

Doherty, P., and K. Gavin. 2011. "Shaft capacity of open-ended piles in clay." *J. Geotech. Geoenviron. Eng.* 137 (11): 1090–1102. https://doi.org/10.1061/(ASCE)GT.1943-5606.0000528.

Doherty, P., and K. Gavin. 2013. "Pile Aging in cohesive soils." *J. Geotech. Geoenviron. Eng.* 139 (9): 1620–1624. https://doi.org/10.1061/(ASCE)GT.1943-5606.0000884.

Doyle, E. H., and J. H. Pelletier. 1985. "Behavior of a Large-Scale Pile in Silty Clay." In *Proc., 11th Int. Conf. on Soil Mechanics and Foundation Engineering*, 1595–1598. Rotterdam: A.A. Balkema.

Ertec. 1982. *Site investigation and soil characterization study at Block 58, West Delta Area, Gulf of Mexico*. Rep. No. 82-200-1. Alameda, CA: Ertec.

Eslami, A., and B. H. Fellenius. 1997. "Pile capacity by direct CPT and CPTu methods applied to 102 case histories." *Can. Geotech. J.* 34 (6): 886–904. https://doi.org/10.1139/t97-056.

Fellenius, B. H., D. E. Harris, and D. G. Anderson. 2004. "Static loading test on a 45 m long pipe pile in Sandpoint, Idaho." *Can. Geotech. J.* 41 (4): 613–628. https://doi.org/10.1139/t04-012.

Fellenius, B. H., and L. Samson. 1976. "Testing of drivability of concrete piles and disturbance to sensitive clay." *Can. Geotech. J.* 13 (2): 139–160. https://doi.org/10.1139/t76-015.

Femern A/S. 2014. *Ground Investigation*. Rep. No. GDR 00.1-001. Copenhagen, Denmark: Ramboll Arup Joint Venture, Ramboll Denmark A/S.

Frank, R. 2017. "Some aspects of research and practice for pile design in France." *Innovation Infrastruct. Solut.* 2 (1): 1–15. https://doi.org/10.1007/s41062-017-0085-4.

Gallagher, K., and H. St John. 1980. "Field scale model studies of piles as anchorages for buoyant platforms." In *Proc., European Offshore Petroleum Conf. and Exhibition*, 334–360. Schiedam, Netherlands: Offshore Energy.

Gavin, K. G., and B. M. Lehane. 2003. "Shaft friction for open-ended piles in sand." *Can. Geotech. J.* 40 (1): 36–45. https://doi.org/10.1139/t02-093.

Gibbs, C., J. McCauley, U. Mirza, and W. Cox. 1993. "Reduction of field data and interpretation of results for axial load tests of two 762mm diameter pipe piles in clay." In *Proc., Conf. Large Scale Pile Test in Clay*, 285–345. London: Thomas Telford.

Heerema, E. 1979. "Pile driving and static load tests on piles in stiff clay." In *Proc., 11th Annual Offshore Technology Conf.* Richardson, TX: Offshore Technology Conference.

Hosseini, M. A., and M. T. Rayhani. 2015. "Evolution of pile shaft capacity over time in soft clays: Case study: Leda clay." In *Proc., GeoQuebec: 68th Canadian Geotechnical Conf.* Edmonton, Canada: Canadian Geotechnical Society.

Huybrechts, N. 2001. "Test campaign at Sint-Katelijne-Waver and installation techniques of screw piles." In *Proc., Symp. on Screw Piles: Screw Piles–Installation and Design in Stiff Clay*, edited by A. Holeyman, 151–176. Boca Raton, FL: CRC Press.

ISO. 1996. *Petroleum and natural gas industries— Specific requirements for offshore structures, part 4: Geotechnical and foundation design considerations*. ISO 19901-4. London: ISO.

Jardine, R., and F. Chow. 1996. *New design methods for offshore piles*. London: Marine Technology Directorate.

Jardine, R., F. Chow, R. Overy, and J. Standing. 2005. *ICP design methods for driven piles in sands and clays*. London: Thomas Telford.

Karlsrud, K. 2012. "Prediction of load-displacement behaviour and capacity of axially loaded piles in clay based on analyses and interpretation of pile load test results." Ph.D. thesis, Dept. of Civil & Environmental Engineering, Norwegian Univ. of Science and Technology.

Karlsrud, K., C. J. F. Clausen, and P. M. Aas. 2005. "Bearing capacity of driven piles in clay, the NGI approach." In *Proc., Int. Symp. on Frontiers Offshore Geotechnics*, 775–782. New York: Taylor & Francis.

Karlsrud, K., S. Hansen, R. Dyvik, and B. Kalsnes. 1993a. "NGI's pile tests at Tilbrook and Pentre—Review of testing procedures and results." In *Proc., Conf. Large-Scale Pile Tests in Clay*, 405–429. London: Thomas Telford.

Karlsrud, K., T. G. Jensen, E. K. W. Lied, F. Nowacki, and A. Simonsen. 2014. "Significant ageing effects for axially loaded piles in sand and clay verified by new field load tests." In *Proc., Offshore Technology Conf. (OTC)*. Richardson, TX: Offshore Technology Conference.

Karlsrud, K., B. Kalsnes, and F. Nowacki. 1993b. "Response of piles in soft clay and silt deposits to static and cyclic axial loading based on recent instrumented pile load tests." In *Proc., Offshore Site Investigation and Foundation Behaviour*, 549–583. Berlin: Springer.

Karlsrud, K.,, and T. Haugen. 1985. "Axial static capacity of steel model piles in over-consolidated clay." In *Proc., 11th Int. Conf. on Soil Mechanics and Foundation Engineering*, 1401–1406. Rotterdam, Netherlands: A.A. Balkema.

Kolk, H., and E. van der Velde. 1996. "A reliable method to determine friction capacity of piles driven into clays." In *Proc., Offshore Technology Conference (OTC)*. Richardson, TX: Offshore Technology Conference.

Konrad, J. M., and M. Roy. 1987. "Bearing capacity of friction piles in marine clay." *Géotechnique* 37 (2): 163–175. https://doi.org/10.1680/geot.1987.37.2.163.

Kou, H. L., W. Z. Diao, T. Liu, D. L. Yang, and S. Horpibulsuk. 2018. "Field performance of open-ended prestressed high-strength concrete pipe piles jacked into clay." *Sensors* 18 (12): 4216. https://doi.org/10.3390/s18124216.

Kraft, L. M., R. P. Ray, and T. Kagawa. 1981. "Theoretical t-z Curves." *J. Geotech. Eng. Div.* 107 (11): 1543–1561. https://doi.org/10.1061/AJGEB6.0001207.

Lambson, M. D., D. G. Clair, D. W. F. Senner, and R. M. Semple. 1993. "Investigation and interpretation of Pentre and Tilbrook Grange soil conditions." In *Proc., Conf. Large-Scale Pile Tests in Clay*, 134–196, London: Thomas Telford.

Lehane, B. M. 1992. "Experimental investigations of pile behaviour using instrumented field piles." Ph.D. thesis, Dept. of Civil Engineering, Imperial College London (University of London).

Lehane, B. M., et al. 2020. "A new CPT-based axial pile capacity design method for driven piles in sand." In *Proc., 5th Int. Symp. Frontiers Offshore Geotechnics*. Hawthorne, NJ: DFI publications.

Lehane, B. M., F. C. Chow, B. M. McCabe, and R. J. Jardine. 2000. "Relationships between shaft capacity of driven piles and CPT end resistance." *Geotech. Eng. ICE* 143 (8): 93–101. https://doi.org/10.1680/geng.2000.143.2.93.

Lehane, B. M., and R. J. Jardine. 1992. "On the residual strength of Bothkennar clay." *Géotechnique* 42 (2): 363–368. https://doi.org/10.1680/geot.1992.42.2.363.

Lehane, B. M., and R. J. Jardine. 1994a. "Displacement-pile behaviour in a soft marine clay." *Can. Geotech. J.* 31 (2): 181–191. https://doi.org/10.1139/t94-024.

Lehane, B. M., and R. J. Jardine. 1994b. "Displacement pile behaviour in glacial clay." *Can. Geotech. J.* 31 (1): 79–90. https://doi.org/10.1139/t94-009.

Lehane, B. M., R. J. Jardine, A. J. Bond, and F. C. Chow. 1994. "The development of shaft resistance on displacement piles in clay." In *Proc., Int. Conf. on Soil Mechanics and Foundation Engineering*, 473–476. Rotterdam, Netherlands: A.A. Balkema.

Lehane, B. M., R. J. Jardine, and B. A. McCabe. 2003. *Pile group tension cyclic loading: Field test programme at Kinnegar N. Ireland*. Research Rep. No. 101. Bootle, UK: Health and Safety Executive.

Lehane, B. M., Y. Li, and R. Williams. 2013. "Shaft capacity of displacement piles in clay using the cone penetration test." *J. Geotech. Geoenviron. Eng.* 139 (2): 253–266. https://doi.org/10.1061/(ASCE)GT.1943-5606.0000749.

Lehane, B. M., J. K. Lim, P. Carotenuto, F. Nadim, S. Lacasse, R. J. Jardine, and B. F. J. van Dijk. 2017. "Characteristics of unified databases for driven piles." In *Proc. 8th Int. Conf. Offshore investigation and Geotechnics: Smarter solutions for offshore developments*, 162–194. London: Society for Underwater Technology.

Li, Y., and B. M. Lehane. 2012. "Insights gained from instrumented centrifuge displacement piles in Kaolin." *Int. J. Geotech. Eng.* 6 (2): 157–161. https://doi.org/10.3328/IJGE.2012.06.02.157-161.

Liew, S. S., S. S. Gue, and Y. C. Tan. 2002. "Design and instrumentation results of a reinforcement concrete piled raft supporting 2500 ton oil storage tank on very soft alluvium deposits." In *Proc., 9th Int. Conf. on Piling and Deep Foundations*, 263–269. Rotterdam, Netherlands: A.A. Balkema.

Liew, S. S., and Y. W. Kowng. 2005. "Design, installation and verification of driven piles in soft ground." In Vol. 1 of *Proc., 11th Int. Conf. of Int.*

Association for Computer Methods and Advances in Geomechanics, Italy: Bologna Patron Ed.

Ma, M. T., and A. E. Holeyman. 2004. "Vibratory driven pile performances in Flanders clay. International prediction event 2003." In *Proc., Cyclic Behaviour of Soils and Liquefaction Phenomena*, 517–522. Boca Raton, FL: CRC Press.

Matsumoto, T., H. Sekiguchi, T. Shibata, and Y. Fuse. 1992. "Performance of steel pipe piles driven in Pleistocene clays." In *Proc., Int. Conf. on the Application of Stress—Wave Theory to Piles*, 293–298. Rotterdam, Netherlands: A.A. Balkema.

McCabe, B. A., and B. M. Lehane. 2006. "Behavior of axially loaded pile groups driven in clayey silt." *J. Geotech. Geoenviron. Eng.* 132 (3): 401–410. https://doi.org/10.1061/(ASCE)1090-0241(2006)132:3(401).

McQueen, W., B. Miller, P. W. Mayne, and S. Agaiby. 2016. "Piezocone dissipation tests at the Canadian Test Site No. 1, Gloucester, Ontario." *Can. Geotech. J.* 53 (5): 884–888. https://doi.org/10.1139/cgj-2015-0090.

Mengé, P. 2001. "Soil investigation results at Sint-Katelijne-Waver (Belgium)." In *Proc., Symp. on Screw Piles: Screw Piles-Installation and Design in Stiff Clay*, edited by A. Holeyman, 19–62. Boca Raton, FL: CRC Press.

Miller, G. A., and A. J. Lutenegger. 1997. "Influence of pile plugging on skin friction in overconsolidated clay." *J. Geotech. Eng.* 123 (6): 525–533. https://doi.org/10.1061/(ASCE)1090-0241(1997)123:6(525).

NGI (Norwegian Geotechnical Institute). 1988a. *Summary, interpretation and analysis of the pile load tests at the Lierstranda test site*. NGI Rep. No. 52523-26. Oslo, Norway: NGI.

NGI (Norwegian Geotechnical Institute). 1988b. *Summary, interpretation and analysis of the pile load tests at the Onsoy test site*. NGI Rep. No. 52523-23. Oslo, Norway: NGI.

NGI (Norwegian Geotechnical Institute). 1989. *Summary and evaluation of NGI's pile tests at Tilbrook Grange*. NGI Rep. No. 885032-2. Oslo, Norway: NGI.

NGI (Norwegian Geotechnical Institute). 2013. *Time Effects on Pile Capacity:Summary and evaluation of pile test results*. NGI Rep. No. 20061251-00-279-R. Oslo, Norway: NGI.

Niazi, F. S., and P. W. Mayne. 2016. "CPTu-based enhanced UniCone method for pile capacity." *Eng. Geol.* 212 (7): 21–34. https://doi.org/10.1016/j.enggeo.2016.07.010.

Paikowsky, S. G., et al. 2004. *Load and resistance factor, design (LFRD) for deep foundations*. Washington, DC: Transport Research Board.

Pelletier, J., and E. Doyle. 1982. "Tension capacity in silty clays–beta pile test." In *Proc., 2nd Int. Conf. on Numerical Methods in Offshore Piling*, 1–19. New York: Wiley.

Ponniah, D. A. 1989. "Instrumentation of a jacked pile." In Vol. 1 of *Proc., Conf on Instrumentation in Geotechnical Engineering*, 207–220. London: Institution of Civil Engineers.

Potts, D. M., and J. P. Martins. 1982. "The shaft resistance of axially loaded piles in clay." *Géotechnique* 32 (4): 269–386. https://doi.org/10.1680/geot.1982.32.4.369.

Powell, J. J. M., and A. P. Butcher. 2003. "Characterisation of a glacial clay till at Cowden, Humberside." In *Characterisation and engineering properties of natural soils*, edited by T. S. Tan, 983–1020. Lisse, Netherlands: Swets & Zeitlinger.

Puech, A., and O. Benzaria. 2013. "Effect of installation mode on the static behaviour of piles in highly overconsolidated Flanders clay." [In French.] In *Proc., 18th Int. Conf. on Soil Mechanics and Geotechnical Engineering*, 2831–2834. Paris: Presses des Ponts.

Randolph, M. F. 2003. "Science and empiricism in pile foundation design." *Géotechnique* 53 (10): 847–875. https://doi.org/10.1680/geot.2003.53.10.847.

Randolph, M. F., and B. S. Murphy. 1985. "Shaft capacity of driven piles in clay." In *Proc., Offshore Technology Conf., Offshore Technology Conf.*, Richardson, TX: Offshore Technology Conference.

Ridgen, W. J., J. J. Pettit, H. D. St John, and T. J. Poskitt. 1979. "Developments in piling for offshore structures." In *Proc., 2nd Int. Conf. on the Behaviour of OffShore Structures*, 279–296. Cranfield, UK: British Hydromechanics Research Association.

Robertson, P. K. 2009. "Interpretation of cone penetration tests—A unified approach." *Can. Geotech. J.* 46 (11): 1337–1355. https://doi.org/10.1139/T09-065.

Robertson, P. K., R. G. Campanella, M. P. Davies, and A. Sy. 1988. "Axial capacity of driven piles in deltaic soils using CPT." In *Proc., Int. Symp. on Penetration Testing; ISOPT-1. 1*, edited by J. De Ruiter, 919–927. Boca Raton, FL: CRC Press.

Robertson, P. K., and C. E. Wride. 1998. "Evaluating cyclic liquefaction potential using the cone penetration test." *Can. Geotech. J.* 35 (3): 442–459. https://doi.org/10.1139/t98-017.

Rocher-Lacoste, F., S. Borel, L. Gianeselli, and S. Po. 2004. "Comparative behaviour and performances of impact and vibratory driven piles in stiff clay." In *Proc., Cyclic Behaviour of Soils and Liquefaction Phenomena*, 533–540. Boca Raton, FL: CRC Press.

Roy, M., R. Blanchet, F. Tavenas, and P. L. Rochelle. 1981. "Behavior of a sensitive clay during pile driving." *Can. Geotech. J.* 18 (1): 67–85. https://doi.org/10.1139/t81-007.

Semple, R. M., W. J. Rigden, M. F. Randolph, and B. S. Murphy. 1984. "Shaft capacity of driven pipe piles in clay." In *Proc., Symp. On Codes and Standards*, 59–79. Reston, VA: ASCE.

Shanghai Xian Dai. 2008. *The research on single piles beaing capacity methods in Shanghai, China*. Shanghai, China: Shanghai Xian Dai Architecural Design (Group).

Shibata, T., H. Sekiguchi, T. Matsumoto, K. Kita, and S. Motoyama. 1989. "Pile driveability assessment by waveform analyses." In *Proc., 12th Int. Conf. on Mechanics and Foundation Engineering*, 1105–1108. Rotterdam: A.A. Balkema.

Teh, C. I., and G. T. Houlsby. 1991. "An analytical study of the cone penetration test in clay." *Géotechnique* 41 (1): 17–34. https://doi.org/10.1680/geot.1992.42.3.529.

Van Dijk, B. F. J., and H. J. Kolk. 2011. "CPT-based design method for axial capacity of offshore piles in clays." In *Proc., Int. Symp. on Frontiers in Offshore Geotechnics II*, 555–560. London: Taylor & Francis.

Wardle, I. F., G. Price, and T. J. Freeman. 1992. "Effect of time and maintained load on the ultimate capacity of piles in stiff clay." In *Proc., Conf. on Piling in Europe*, 92–99. London: Institution of Civil Engineers.

Whittle, A. J. 1991. *Predictions of instrumented pile behaviour at the Bothkennar site*. London: Imperial College London.

Whittle, A. J., and M. M. Baligh. 1988. *A model for predicting the performance of TLP piles in clays*. Cambridge, MA: Massachusetts Institute of Technology.

Xu, X., H. Liu, and B. M. Lehane. 2006. "Pipe pile installation effects in soft clay." *Proc. Inst. Civ. Eng. Geotech. Eng.* 159 (4): 285–296. https://doi.org/10.1680/geng.2006.159.4.285.